APPLICATION OF THE GUMBEL DISTRIBUTION FOR

MEDICAL ULTRASOUND IMAGE ENHANCEMENT

SARUTA CHONG-NGAM

A Thesis Submitted in Partial Fulfillment of the Requirements for the

Degree of Master of Science in Applied Mathematics

Suranaree University of Technology

Academic Year 2024

การประยุกต์ใช้การแจกแจงกัมเบลสำหรับ
การปรับปรุงภาพถ่ายคลื่นเสียงความถี่สูงทางการแพทย์

นางสาวศรุตา จงงาม

วิทยานิพนธ์นี้เป็นส่วนหนึ่งของการศึกษาตามหลักสูตรปริญญาวิทยาศาสตรมหาบัณฑิต
สาขาวิชาคณิตศาสตร์ประยุกต์
มหาวิทยาลัยเทคโนโลยีสุรนารี
ปีการศึกษา 2567

APPLICATION OF THE GUMBEL DISTRIBUTION FOR MEDICAL

ULTRASOUND IMAGE ENHANCEMENT

Suranaree University of Technology has approved this thesis submitted in partial fulfillment of the requirements for a Master's Degree.

Thesis Examining Committee

_____

(Assoc. Prof. Dr. Pisamai Kittipoom)

Chairperson

_____

(Asst. Prof. Dr. Jessada Tanthanuch)
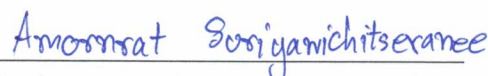
Member (Thesis Advisor)

_____

(Assoc. Prof. Dr. Eckart Schulz)

Member (Thesis Co-Advisor)

_____

(Asst. Prof. Dr. Tidarut Areerak)

Member

_____

(Dr. Amornrat Suriyawichitseranee)

Member

_____

(Assoc. Prof. Dr. Yupaporn Ruksakulpiwat)

Vice Rector for Academic Affairs

and Quality Assurance

_____

(Prof. Dr. Santi Maensiri)

Dean of Institute of Science

ศรุตา จงงาม : การประยุกต์ใช้การแจกแจงกัมเบลสำหรับการปรับปรุงภาพถ่ายคลื่นเสียง
ความถี่สูงทางการแพทย์ (APPLICATION OF THE GUMBEL DISTRIBUTION FOR MEDICAL
ULTRASOUND IMAGE ENHANCEMENT) อาจารย์ที่ปรึกษา : ผู้ช่วยศาสตราจารย์ ดร.
เจษฎา ตัณฑนุช, 61 หน้า.

คำสำคัญ: ภาพถ่ายคลื่นเสียงความถี่สูงทางการแพทย์/การลดสัญญาณรบกวน/การแจกแจงทางสถิติ
กัมเบล/แคลคูลัสของการแปรผัน

วิทยานิพนธ์นี้ต้องการพัฒนาตัวแบบทางคณิตศาสตร์เพื่อใช้ในการลดทอนสัญญาณรบกวนที่
ปรากฏในภาพถ่ายคลื่นเสียงความถี่สูงทางการแพทย์ สำหรับการสร้างตัวแบบในครั้งนี้จะพิจารณาว่า
สัญญาณรบกวนที่ปรากฏในขั้นตอนการสร้างภาพเป็นการแจกแจงทางสถิติเรย์ลีและเมื่อนำไปสู่
ขั้นตอนประมวลผลภาพจากสุดท้ายเพื่อแสดงผลออกมา สัญญาณรบกวนมีการแจกแจงทางสถิติ
กัมเบล การสร้างตัวแบบจะเริ่มจากตัวแบบวิยุตแล้วพัฒนาต่อไปสู่ตัวแบบต่อเนื่องในรูปแบบเชิง
อินทิกรัลแล้วใช้แคลคูลัสของการแปรผันเพื่อพัฒนาตัวแบบให้อยู่ในรูปแบบสมการเชิงอนุพันธ์ ใน
ด้านการทดสอบประสิทธิภาพของตัวแบบได้พัฒนาโปรแกรมภาษาไพทอนเพื่อใส่สัญญาณรบกวนที่มี
การแจกแจงทางสถิติกัมเบลบนรูปเลนาที่เป็นมาตรฐาน จากนั้นพัฒนาโปรแกรมภาษาไพทอนเพื่อทำ
การลดสัญญาณรบกวนด้วยตัวแบบที่พัฒนาขึ้นและวิธีเชิงตัวเลข ทำการประเมินประสิทธิภาพโดยใช้
ค่าความแตกต่างสัมบูรณ์ (เอดี), ค่าความคลาดเคลื่อนกำลังสองเฉลี่ย (อาร์เอ็มเอสอี), ค่าสัมประสิทธิ์
สหสัมพันธ์ (ซีโออาร์อาร์) และดัชนีคุณภาพสากล (ยูคิวไอ)

สาขาวิชาคณิตศาสตร์และภูมิสารสนเทศ ลายมือชื่อนักศึกษา _ศรุตา จงงาม_
ปีการศึกษา 2567 ลายมือชื่ออาจารย์ที่ปรึกษา _J. Tanthanuch_
ลายมือชื่ออาจารย์ที่ปรึกษาร่วม _____

SARUTA CHONG-NGAM : APPLICATION OF THE GUMBEL DISTRIBUTION FOR MEDICAL ULTRASOUND IMAGE ENHANCEMENT. THESIS ADVISOR : ASST. PROF. JESSADA TANTHANUCH, Ph.D. 61 PP.

Keyword: MEDICAL ULTRASOUND IMAGE, NOISE REDUCTION, GUMBEL DISTRIBUTION, CALCULUS OF VARIATIONS

This thesis aims to develop a mathematical model for noise reduction in high-frequency ultrasound medical imaging. In constructing this model, the noise that arises during the image formation process is assumed to follow a Rayleigh statistical distribution. When the image undergoes final processing for visualization, the noise is assumed to follow a Gumbel statistical distribution. The model development begins with a discrete formulation and is subsequently extended to a continuous form using an integral-based approach. Variational calculus is then applied to refine the model into a differential equation representation. For performance evaluation, a Python program was developed to introduce Gumbel distributed noise into standardized test images. Another Python program was then implemented to perform noise reduction using the proposed model and numerical methods. The effectiveness of the model was assessed using absolute difference (AD), root mean square error (RMSE), correlation coefficient (Corr), and universal quality index (UQI).

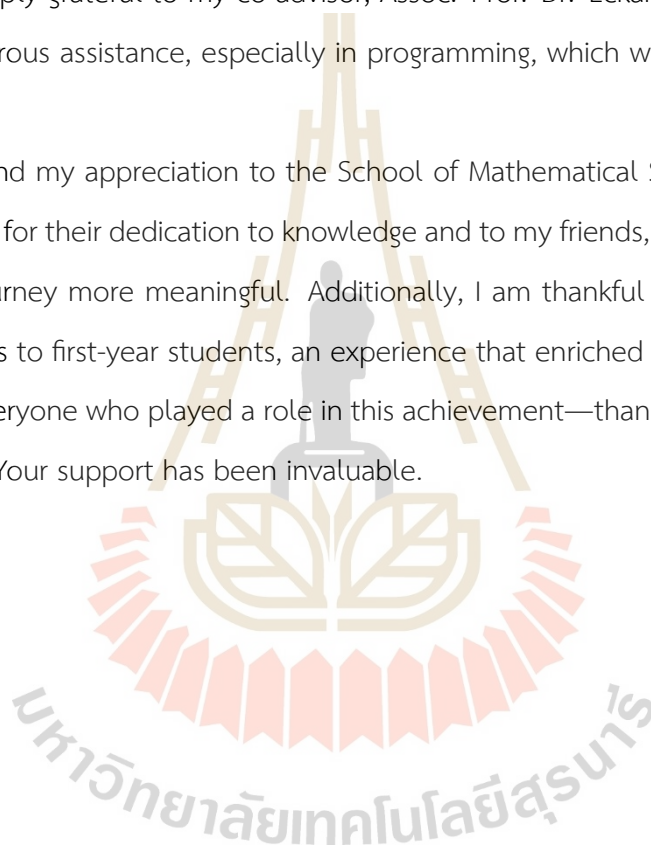|	
School of Mathematical Sciences	Student's Signature _____
and Geoinformatics	Advisor's Signature _____
Academic Year 2024	Co-Advisor's Signature _____

ACKNOWLEDGEMENTS

I sincerely thank my advisors for their unwavering guidance and support throughout this journey. My deepest gratitude goes to Asst. Prof. Dr. Jessada Tanthanuch, whose invaluable insights and encouragement shaped both my research and academic growth. I am also deeply grateful to my co-advisor, Assoc. Prof. Dr. Eckart Schulz, for his expertise and generous assistance, especially in programming, which was fundamental to this thesis.

I extend my appreciation to the School of Mathematical Sciences and Geoinformatics at SUT for their dedication to knowledge and to my friends, whose companionship made this journey more meaningful. Additionally, I am thankful for the opportunity to teach calculus to first-year students, an experience that enriched my academic path.

To everyone who played a role in this achievement—thank you from the bottom of my heart. Your support has been invaluable.

Saruta Chong-Ngam

CONTENTS

CONTENTS (Continued)

CONTENTS (Continued)

LIST OF TABLES

LIST OF FIGURES

CHAPTER I

INTRODUCTION

In the contemporary landscape of medical diagnostics, ultrasound imaging stands as a cornerstone technology due to its non-invasive nature, real-time imaging capabilities, and widespread accessibility. Despite these advantages, the quality of ultrasound images is frequently compromised by the presence of speckle noise, which can obscure critical anatomical details and hinder accurate clinical interpretation. Consequently, there is an ongoing quest within the medical imaging community to develop sophisticated techniques for speckle noise reduction, thereby enhancing image quality and diagnostic reliability.

There are several techniques for image noise reduction. One well-known method, introduced by Rudin, Osher, and Fatemi (1992), is based on a constrained optimization approach using calculus of variations. This method minimizes noise while preserving edges and details in the image. In addition to denoising, it can be applied to image restoration tasks such as deblurring and demosaicing. This technique is noninvasive, meaning it does not introduce new artifacts or distortions into the image, thereby preserving sharp edges and details. Moreover, the algorithm is relatively fast and simple to implement.

Statistical modeling has been instrumental in improving ultrasound image quality, particularly through the application of Rayleigh and Gumbel distributions. These distributions have been widely utilized to address challenges in speckle noise reduction, boundary detection, and contrast enhancement, which are critical for accurate medical diagnoses. Booth and Li (2007) introduced a segmentation technique based on the Gumbel distribution, designed to overcome the limitations of conventional gradient- and intensity-based methods, which often struggle with weak or low-contrast edges. Their approach involved decomposing B-mode images into A-mode scans, which allowed for a more structured analysis of pixel intensity variations. They used the Expectation-Maximization (EM) algorithm to repeatedly estimate the parameters of the Gumbel distribution, which resulted in enhanced boundary identification accuracy across various ultrasound datasets.

Around the same period, Seekot (2008) extended the variational approach for ultrasound image enhancement, integrating a combination of the Rayleigh distribution, Euler-Lagrange equations, and the ROF model. The Rayleigh distribution, widely used for modeling backscattered signals, was incorporated into the variational framework to optimize noise suppression while preserving essential anatomical structures. The Euler-Lagrange equations facilitated the derivation of energy-minimizing solutions, ensuring that the enhancement process retained the most relevant image features. Additionally, the ROF model, a fundamental technique in variational image denoising, was employed to balance speckle noise reduction and edge preservation. Building on these concepts, Tan-thanuch et al. (2012, 2015) further advanced variational denoising models by explicitly incorporating Rayleigh-distributed speckle noise. Their approach introduced adaptive noise reduction techniques, ensuring significant suppression of noise while preserving anatomical fidelity, a crucial factor for improving the clinical utility of ultrasound images. These advancements demonstrated the effectiveness of probabilistic models and variational calculus in enhancing ultrasound imaging accuracy and quality.

More recent developments have focused on refining these statistical models to enhance their adaptability, robustness, and performance across different imaging conditions. Bashir and Rasul (2018) introduced the Area-Biased Rayleigh Distribution (ARD), an extension of the standard Rayleigh model designed to address sampling biases and incomplete observations, particularly in low-quality ultrasound datasets. Expanding on this, Ateeq, Qasim, and Alvi (2019) proposed the Rayleigh-Rayleigh Distribution (RRD), which incorporated additional shape parameters to provide greater flexibility in modeling complex ultrasound data distributions. By introducing a secondary Rayleigh component, this model improved the representation of heterogeneous tissue structures, making it particularly useful in distinguishing healthy and pathological tissues. Further advancements were made with the Power Rayleigh (PR) distribution (Mahmoud et al., 2020), which optimized noise characterization in both medical and environmental imaging applications, offering improved modeling of speckle noise intensities under varying imaging conditions.

Beyond ultrasound imaging, exponential-based statistical models have also been explored for their potential in noise filtering and feature extraction. Notable among these

are the Transmuted Topp-Leone Exponential (TTLE) model (Almutiry et al., 2021) and the Unit Exponential Distribution (UED) (Bakouch et al., 2023), which have been applied to model skewed and bounded data distributions in medical images, where intensity values often exhibit non-symmetric patterns. Hashim et al. (2024) further contributed by introducing the Modified Exponential Distribution Optimizer (mEDO), incorporating Phasor Operators and Adaptive p-best Mutation Strategies to enhance global optimization and multi-level thresholding for ultrasound image segmentation.

In recent years, many noise reduction methods have favored deep learning techniques, often employing black-box approaches (Takagi and Koseki, 2022; Mansouri et al., 2022). However, these methods typically lack detailed explanations beyond their use of computer-based algorithms. This thesis aims to develop a noise reduction model for medical ultrasound images by applying the Gumbel distribution in conjunction with the calculus of variations, following the approach introduced by Rudin, Osher, and Fatemi (1992). The research includes analyzing various properties of the proposed model and assessing its effectiveness in reducing noise. Understanding this model will enhance our ability to explain phenomena observed in the ultrasound imaging process.

1.1   Research objective

1. To develop an efficient image enhancement method for medical ultrasound images using the Gumbel distribution to improve the quality of medical ultrasound images.

2. To investigate the effectiveness of using the Gumbel distribution in enhancing medical ultrasound images to improve their quality for better diagnosis and interpretation.

1.2   Scope and limitations

1. The images used in this thesis are ultrasound medical digital grayscale image.

2. Main software used for working in the thesis is Python.

1.3   Research procedure

The research work will proceed as follows:

1. Investigate and understand the mathematical principles of Gumbel distribution, focusing on their application in medical ultrasound image enhancement.

2. Explore techniques used in medical ultrasound image enhancement to improve the quality of ultrasound images, such as noise reduction, sharpness enhancement, and brightness adjustment.

3. Develop Python programs to perform ultrasound image enhancement using the studied techniques and the Gumbel distribution.

4. Utilize the enhanced ultrasound images from the previous steps for evaluation and analysis. Measure the effectiveness of image enhancement methods and compare results with other techniques.

5. Summarize the research findings and analysis results. Emphasize the suitability of the Gumbel distribution and propose future research directions to further improve medical ultrasound image enhancement.

1.4   Expected result

1. Development of a methodology for enhancing medical digital ultrasound images using the Gumbel distribution.

2. Comprehensive performance evaluation of the proposed enhancement method.

CHAPTER II

LITERATURE REVIEW

This section presents knowledge about statistical distributions and the calculus of variations, which are essential for enhancing the quality of medical ultrasound images. Furthermore, related research will be reviewed in order to improve this research process and achieve more efficient results.

2.1 Digital Image

A digital image refers to an image that has been transformed into digital data, consisting of numerous pixels, each with distinct color and brightness values (Gonzalez and Woods, 2018).

Medical images, including X-rays, ultrasounds, and MRIs, are digital images utilized for the diagnosis and treatment of diseases. These images are produced through advanced medical technologies and subsequently converted into digital format to facilitate computer-based processing and analysis.

Thus, medical images represent a specific category of digital images employed in the medical field to support the diagnosis and treatment of diseases. Converting these images into digital format enables efficient processing and analysis by computers, providing substantial benefits to medical practice.

2.2 Medical Ultrasound Image

Medical ultrasound imaging is a medical imaging technique that uses high-frequency sound waves to create images of structures inside the body. It is a crucial aspect of medical diagnosis, offering several advantages such as real-time imaging, low cost, and non-invasive procedures. However, ultrasound images often contain significant

noise and artifacts, making image processing and enhancement essential for diagnostic accuracy.

2.3   Calculus of Variations

Calculus of variations is a part of mathematics that finds the best function to maximize or minimize an expression called a functional, which involves the function and its derivatives. The goal is to find the best path, curve, surface, or function that makes this expression as large or as small as possible.

Mathematically, this involves finding a function $y(x)$ that makes the integral

$$I = \int_{x_1}^{x_2} F(x, y, y') \, dx,$$

extremal, where F is a given function. The procedure involves considering a family of varied curves given by

$$\tilde{y}(x) = y(x) + \epsilon \eta(x),$$

where $\eta(x)$ is an arbitrary function satisfying $\eta(x_1) = \eta(x_2) = 0$. Then,

$$I(\epsilon) = \int_{x_1}^{x_2} F(x, \tilde{y}(x), \tilde{y}'(x)) \, dx.$$

We require $\dfrac{d}{d\epsilon} I(\epsilon) = 0$ when $\epsilon = 0$. Recognizing that $\tilde{y}$ and $\tilde{y}'$ are functions of ϵ, and differentiating under the integral sign with respect to ϵ, we obtain

$$\frac{d}{d\epsilon} I(\epsilon) = \int_{x_1}^{x_2} \left(\frac{\partial F}{\partial \tilde{y}} \frac{d\tilde{y}}{d\epsilon} + \frac{\partial F}{\partial \tilde{y}'} \frac{d\tilde{y}'}{d\epsilon} \right) dx.$$

Substituting $\tilde{y}(x) = y(x) + \epsilon \eta(x)$ and $\tilde{y}'(x) = y'(x) + \epsilon \eta'(x)$, and evaluating at $\epsilon = 0$, we have

$$\left. \frac{d}{d\epsilon} I(\epsilon) \right|_{\epsilon=0} = \int_{x_1}^{x_2} \left(\frac{\partial F}{\partial y} \eta(x) + \frac{\partial F}{\partial y'} \eta'(x) \right) dx = 0.$$

Assuming $\eta(x)$ and its derivatives are continuous, we can integrate the second term by parts:

$$\int_{x_1}^{x_2} \frac{\partial F}{\partial y'} \eta'(x) \, dx = \left. \frac{\partial F}{\partial y'} \eta(x) \right|_{x_1}^{x_2} - \int_{x_1}^{x_2} \frac{d}{dx} \left(\frac{\partial F}{\partial y'} \right) \eta(x) \, dx.$$

Since $\eta(x) = 0$ at x_1 and x_2, the boundary term vanishes, yielding:

$$\int_{x_1}^{x_2} \left(\frac{\partial F}{\partial y} - \frac{d}{dx} \left(\frac{\partial F}{\partial y'} \right) \right) \eta(x) \, dx = 0.$$

As $\eta(x)$ is arbitrary, we must have:

$$\frac{\partial F}{\partial y} - \frac{d}{dx} \left(\frac{\partial F}{\partial y'} \right) = 0.$$

This is the Euler equation (or Euler-Lagrange equation). To solve any problem in the calculus of variations, we establish the integral to be stationary, determine the function F, substitute it into the Euler equation, and solve the resulting differential equation (Boas, 2006).

2.4   Statistical Distributions

Distributions are important tools in statistics and probability theory that are used to describe the distribution of data of interest. In the field of medical ultrasound imaging, understanding and modeling the statistical distributions of image data is crucial for various applications, including image enhancement, segmentation, and classification. The following are some common statistical distributions that are typically used in the analysis and processing of ultrasound images.

2.4.1   Exponential Distribution

The exponential distribution is a continuous probability distribution widely used to model the time between events in a Poisson process. It is characterized by a single parameter $\lambda > 0$, representing the rate of occurrence. The probability density function (pdf) of the Exponential distribution is

$$f(x; \lambda) = \begin{cases} \lambda e^{-\lambda x}, & x \geq 0, \\ 0, & x < 0. \end{cases}$$

The Exponential distribution is known for its "memoryless property", meaning that the probability of an event occurring in the future is independent of the past. It has a mean of $\frac{1}{\lambda}$ and a variance of $\frac{1}{\lambda^2}$. (Krishnamoorthy, 2006)

The Exponential distribution is applied in medical imaging to model phenomena such as signal attenuation in ultrasound or decay of tracer signals in nuclear medicine. It simplifies noise modeling and improves the quantitative analysis of imaging data.

2.4.2 Rayleigh Distribution

The Rayleigh distribution is a continuous probability distribution commonly used to model the magnitude of a two-dimensional vector with independent Gaussian components. It is defined by a single scale parameter $\sigma > 0$. The pdf of the Rayleigh distribution is

$$f(x; \sigma) = \begin{cases} \frac{x}{\sigma^2} e^{-\frac{x^2}{2\sigma^2}}, & x \geq 0, \\ 0, & x < 0. \end{cases}$$

The Rayleigh distribution has a mean of $\sigma\sqrt{\frac{\pi}{2}}$ and a variance of $\frac{(4-\pi)\sigma^2}{2}$. (Krishnamoorthy, 2006)

In medical imaging, the Rayleigh distribution is often applied to model the intensity of backscattered ultrasound signals in regions where no strong reflectors exist. It is also effective in analyzing and reducing speckle noise, enhancing image quality for better diagnostic accuracy.

2.4.3 Gumbel Distribution

The Gumbel distribution is a continuous probability distribution used to model the distribution of the maximum (or minimum) of a number of samples from various distributions. It is characterized by two parameters: the location parameter μ and the scale parameter $\beta > 0$. The pdf of the Gumbel distribution is

$$f(x; \mu, \beta) = \frac{1}{\beta} \exp\left[\frac{x - \mu}{\beta}\right] \exp\left[-e^{\frac{x-\mu}{\beta}}\right], \quad -\infty < x < \infty.$$

The Gumbel distribution has a mean of $\mu - \beta\gamma$ and a variance of $\frac{\pi^2\beta^2}{6}$, where γ is the Euler-Mascheroni constant (NIST/SEMATECH, 2012).

In medical imaging, the Gumbel distribution is applied to model extreme values, such as the maximum intensities of signals in specific regions. This is particularly useful in

the analysis of tissue abnormalities or in scenarios requiring the modeling of peak signal responses. Its ability to handle extremes makes it valuable in detecting outliers and anomalies in imaging data.

2.5 Tools for Evaluation the Models

For performance evaluation of the proposed method in the context of medical ultrasound images, several quantitative measures have been selected to ensure a comprehensive assessment of image quality and fidelity. These measures are crucial for determining the effectiveness of the model in enhancing ultrasound images, which are often affected by various types of noise and distortions. The chosen metrics include Absolute Difference (AD), Root Mean Square Error (RMSE), Correlation Coefficient (Corr), and Universal Quality Index (UQI)

2.5.1 Absolute Difference (AD)

The absolute difference (AD) is a simple yet effective metric for measuring the difference between the original and processed images. It is calculated as

$$AD = \frac{1}{N} \sum_{i=1}^{N} |x_i - y_i|,$$

where

x_i and y_i are pixel values from the original and processed images, respectively,

N is the total number of pixels in the image.

The absolute difference quantifies the pixel-wise deviation between the original and denoised images. A lower AD value indicates that the processed image is more similar to the original, meaning less distortion was introduced by the enhancement process. Absolute Difference is particularly useful for detecting artifacts introduced by image processing methods and ensuring that the model does not remove critical diagnostic information while reducing noise (Gonzalez and Woods, 2018).

2.5.2 Root Mean Square Error (RMSE)

The root mean square error (RMSE) is a standard metric for measuring the overall error between the original and processed images. It is calculated as

$$RMSE = \sqrt{\frac{1}{N} \sum_{i=1}^{N} (x_i - y_i)^2},$$

where x_i and y_i are pixel values from the original and processed images, respectively, N is the total number of pixels in the image. RMSE provides a measure of the average magnitude of error, taking into account both the variance and bias of the processed image compared to the original. A lower RMSE value indicates that the model introduces minimal distortion while enhancing image quality. This metric is particularly useful for evaluating the noise reduction capability of the model, as it emphasizes larger deviations between the original and processed images (Gonzalez and Woods, 2018).

2.5.3 Correlation Coefficient (Corr)

The correlation coefficient (Corr) is a widely used metric that quantifies the similarity between the original and processed images. It is computed as

$$\rho = \frac{\sum (x_i - \mu_x)(y_i - \mu_y)}{\sqrt{\sum (x_i - \mu_x)^2 \sum (y_i - \mu_y)^2}},$$

where

x_i and y_i are pixel values from the original and processed images, respectively,

μ_x and μ_y are the mean values of the original and processed images, respectively.

The correlation coefficient ranges from -1 to 1,

where

$\rho = 1$ indicates a perfect positive correlation (high similarity),

$\rho = 0$ indicates no correlation,

$\rho = -1$ indicates a perfect negative correlation.

A higher correlation coefficient value (close to 1) suggests that the processed image retains the original structure, implying that the model has effectively enhanced the image without distorting essential diagnostic features (Gonzalez and Woods, 2018).

2.5.4 Universal Quality Index (UQI)

The universal quality index (UQI) is another critical metric employed for image quality assessment. It is given by (Zhou et al., 2002)

$$UQI = \frac{4\xi_{xy}\mu_x\mu_y}{\left(\xi_x^2 + \xi_y^2\right)\left(\mu_x^2 + \mu_y^2\right)},$$

where

ξ_x and ξ_y are the standard deviations of image intensity for each pixel of images x and y, respectively,

ξ_{xy} is the covariance of images x and y, comparing pixel by pixel,

μ_x and μ_y are the means of the image intensity of image x and y, respectively.

The universal quality index was designed by modeling any image distortion as a combination of three factors: loss of correlation, luminance distortion, and contrast distortion. This makes it particularly well-suited for evaluating images with nonuniform noise, such as those produced by ultrasound equipment. Ultrasound images often suffer from speckle noise, which can obscure important diagnostic details. By using universal quality index, we can measure how well the proposed model preserves important image features while reducing unwanted noise and distortions.

The application of these quantitative measures to medical ultrasound images allows for a rigorous assessment of the proposed model's performance. By focusing on absolute difference, root mean square error, correlation coefficient, and universal quality index, we ensure that the evaluation covers pixel-wise accuracy, structural similarity, and overall image fidelity. This approach provides a comprehensive insight into the model's effectiveness in reducing noise while preserving essential diagnostic information. Such an assessment is crucial for enhancing the diagnostic utility of ultrasound imaging, ultimately contributing to more accurate medical evaluations and improved patient outcomes.

2.6   Related Researches

Rudin, Osher, and Fatemi (1992) introduced the Rudin-Osher-Fatemi (ROF) model, a groundbreaking technique in image processing that employs Total Variation (TV) calculus

to reduce noise while preserving important image features such as edges. This capability is particularly beneficial in medical imaging. The ROF model formulates denoising as an optimization problem, minimizing an energy functional that balances a fidelity term (ensuring the denoised image remains close to the original) and a regularization term (promoting smoothness by minimizing total variation). This approach effectively reduces noise without overly smoothing the image, thereby maintaining critical details essential for accurate diagnosis and analysis. Despite the computational intensity and the challenge of selecting an appropriate regularization parameter, the ROF model's edge-preserving capability and flexibility have made it a foundational technique in image processing, significantly enhancing the quality of medical images.

Booth and Li (2007) introduced a Gumbel distribution-based method for boundary detection in ultrasound image segmentation, addressing limitations of traditional gradient- and intensity-based approaches. By decomposing B-mode images into A-mode scans and modeling intensity patterns with Gumbel distributions using Expectation-Maximization, their method achieved superior accuracy. Tests on 304 in vivo pork loin ultrasound images showed stronger alignment with expert-traced contours and fewer outliers, demonstrating the method's effectiveness in enhancing segmentation accuracy for medical and agricultural applications.

Seekot (2008) extended the variational approach for ultrasound image enhancement in his master's thesis. The study delved deeper into the theoretical framework, including the Rayleigh distribution, Euler-Lagrange equations, and the use of the Rudin-Osher-Fatemi (ROF) model as a foundation. The thesis presented a comprehensive analysis of the variational functional used for optimization, integrating both regularization and data fidelity terms. The approach was tested using both synthetic and real-world ultrasound images, with results showing significant improvements in noise reduction. The thesis also included the development of prototype software for implementing and evaluating the proposed method.

Tanthanuch, Seekot and Schulz (2012) proposed a variational approach for reducing speckle noise in ultrasound images, caused by the scattering of ultrasonic waves on rough surfaces and statistically modeled using the Rayleigh distribution. The approach

utilized the calculus of variations to develop a denoising model, transforming the problem into an Euler-Lagrange equation and solving it numerically with the gradient descent method. Experimental validation using synthetic and real images, such as the Lena image, demonstrated the model's effectiveness in reducing noise while preserving image details. The high correlation coefficients between the original and reconstructed images further confirmed its performance.

Tanthanuch and Schulz (2015) developed a variational model to reduce speckle noise in medical ultrasound images, based on the Rayleigh distribution. The model uses calculus of variations to minimize a functional that balances noise reduction with detail preservation. The research proved the existence and uniqueness of solutions and solved the model using gradient descent. Tests on standard and ultrasound images showed the model outperformed existing methods, such as the ROF, Le, and AA models, by reducing noise effectively while maintaining image structure.

Bashir and Rasul (2018) proposed the Area-Biased Rayleigh Distribution (ARD) as an improved extension of the classical Rayleigh Distribution (RD) for modeling lifetime data, particularly in scenarios involving sampling biases or incomplete observations. They thoroughly derived its mathematical properties, including moments, skewness, kurtosis, and entropy, and demonstrated its effectiveness through parameter estimation methods such as the Method of Moments (MOM), Maximum Likelihood Estimation (MLE), and Bayesian estimation, with MLE achieving the Cramer-Rao Lower Bound, which ensures minimum variance for unbiased estimators. The ARD was applied to datasets on patient relief times and aircraft window strength, where it outperformed other distributions, as confirmed by the Kolmogorov-Smirnov test (K-S test). Its smoother survival function and gradually increasing hazard rate underscored its suitability for reliability and medical applications, establishing it as a flexible and robust alternative to existing models.

Ateeq, Qasim and Alvi (2019) developed the Rayleigh-Rayleigh Distribution (RRD), an improved version of the Rayleigh Distribution (RD). This new model adds extra parameters to better handle complex data, making it more accurate than other similar models. The researchers explained how the RRD works, including its key features like probability calculations and reliability measures. They tested it using real-world data, such as pa-

tient survival times and material strengths, and showed it fits better than existing models. Their work highlights the RRD's usefulness in fields like medical imaging and engineering for analyzing and understanding complex patterns in data.

Mahmoud et al. (2020) introduced the Power Rayleigh (PR) distribution, a two-parameter extension of the Rayleigh model, designed to improve flexibility in statistical analysis. The PR distribution's statistical properties, including its probability density, hazard rate, and moments, were thoroughly explored. Using maximum likelihood estimation (MLE) and simulations, the authors validated the distribution's robustness. Applied to hydrological runoff data, the PR model outperformed alternatives like the Gumbel and Pareto distributions, based on goodness-of-fit metrics such as AIC and BIC. The study demonstrated the PR distribution's adaptability and effectiveness in reliability and environmental data modeling, establishing it as a valuable tool in these fields.

Almutiry et al. (2021) introduced the "Transmuted Topp-Leone Exponential (TTLE)" model, a three-parameter statistical distribution tailored for medical data analysis. By accommodating skewed, unimodal, and decreasing distributions, the model effectively captures survival and reliability patterns common in clinical datasets. When applied to "Guinea Pig survival data", the TTLE model demonstrated precision in modeling survival variations, making it highly suitable for analyzing patient outcomes and disease progression. Using Maximum Likelihood Estimation (MLE) in "MATHCAD 14", the TTLE model outperformed alternatives like the Beta Exponential and Exponentiated Weibull distributions, showcasing its adaptability and accuracy. Overall, the TTLE model provides a flexible and robust framework for survival data analysis, with promising applications in clinical research, diagnostics, and treatment planning.

Bakouch et al. (2023) introduced the Unit Exponential Distribution (UED), a flexible two-parameter model for proportional data, offering improved versatility over traditional distributions like Beta and Kumaraswamy. The UED's key features include its ability to handle positive and negative skewness and its consistent increasing failure rate (IFR). Parameters were estimated using Maximum Likelihood Estimation (MLE), validated through simulations. Goodness-of-fit tests, including Kolmogorov–Smirnov and Anderson–Darling, confirmed UED's superior performance. Applied to soil moisture and burr measurements,

the UED consistently outperformed alternatives, supported by metrics like AIC and BIC. The UED stands out as a robust and adaptable model for bounded data.

Hashim et al. (2024) introduced an enhanced version of the Exponential Distribution Optimizer (EDO), named the Modified Exponential Distribution Optimizer (mEDO), designed to address global optimization and multi-level thresholding problems in image segmentation. The mEDO incorporates two novel strategies: the Phasor Operator, which improves the exploration capability by employing periodic trigonometric functions, and the Adaptive p-best Mutation Strategy, which enhances exploitation and prevents convergence to local optima.

CHAPTER III

RESEARCH METHODOLOGY

This section presents the research methodology employed in developing a statistical model for enhancing medical ultrasound images. The study focuses on deriving the probability density function (PDF), modeling log-compressed image intensities, and proposing a noise reduction model using the Gumbel distribution. The methodology involves the following steps:

1. Derivation of the PDF,

2. Modeling of a log-compressed image,

3. The Proposed Model.

3.1 Derivation of the Probability Density Function

In general, let X be a continuous random variable with probability density function (PDF) $f_X(x)$ supported on an interval (c, ∞). (i.e., $f_X(x) = 0$ for $x \leq c$). Next, let $h : (c, \infty) \to \mathbb{R}$ be increasing, continuous and one-to-one and onto. Set

$$Y := h \circ X.$$

We want to compute the PDF of this new random variable Y. Recall that the CDF of X is

$$F_X(t) = P(X \leq t) = \int_c^t f_X(\tau)\, d\tau \quad (t > c),$$

and $F_X(t) = 0$ for $t \leq c$. Thus the CDF of Y is

$$F_Y(y) = P(Y \leq y) = P(h(X) \leq y)$$

$$= P(X \leq h^{-1}(y)) = F_X(h^{-1}(y))$$

$$= \int_c^{h^{-1}(y)} f_X(\tau)\, d\tau \quad (y \in \mathbb{R}).$$

Consequently, the PDF of Y is

$$f_Y(y) = \frac{d}{dy} \int_c^{h^{-1}(y)} f_X(\tau)\, d\tau = f_X(h^{-1}(y))(h^{-1})'(y).$$

Now assume that X is a Rayleigh-distributed random variable. So its density function (PDF) is

$$f_X(x) = \frac{x}{\sigma^2} e^{-x^2/(2\sigma^2)}, \quad (x \geq 0).$$

Next choose $h(x) = a \ln x + b$, i.e.

$$Y = a \ln X + b, \tag{3.1}$$

where a, b are constants, $a > 0$. Then $h^{-1}(y) = \exp\left[\frac{y-b}{a}\right]$ for $y \in \mathbb{R}$.

By the above, the PDF of Y is

$$\begin{aligned}
f_Y(y) &= f_X(h^{-1}(y))(h^{-1})'(y) \\
&= \frac{\exp\left[\frac{y-b}{a}\right]}{\sigma^2} \exp\left[-\left(e^{\frac{y-b}{a}}\right)^2 /(2\sigma^2)\right] \exp\left[\frac{y-b}{a}\right] \frac{1}{a} \\
&= \frac{1}{a\sigma^2} \exp\left[-e^{2\left(\frac{y-b}{a}\right)}/(2\sigma^2)\right] \exp\left[2\frac{y-b}{a}\right], \quad (y \in \mathbb{R}).
\end{aligned}$$

We now simplify this formula. First set $\beta = \frac{a}{2}$. We get

$$f_Y(y) = \frac{1}{2\beta\sigma^2} \exp\left[-e^{\frac{y-b}{\beta}}/(2\sigma^2)\right] \exp\left[\frac{y-b}{\beta}\right].$$

Because $2\sigma^2 = e^{\ln(2\sigma^2)}$, then

$$\begin{aligned}
f_Y(y) &= \frac{1}{\beta \exp[\ln(2\sigma^2)]} \exp\left[-e^{\frac{y-b}{\beta}}/e^{\ln(2\sigma^2)}\right] \exp\left[\frac{y-b}{\beta}\right] \\
&= \frac{1}{\beta} \exp\left[-e^{\frac{y-b}{\beta}-\ln(2\sigma^2)}\right] \exp\left[\frac{y-b}{\beta} - \ln(2\sigma^2)\right].
\end{aligned}$$

Setting $\alpha = \beta \ln(2\sigma^2) + b$, this becomes

$$f_Y(y) = \frac{1}{\beta} \exp\left[-e^{\frac{y-\alpha}{\beta}}\right] \exp\left[\frac{y-\alpha}{\beta}\right],$$

so that if $g = \frac{\alpha-y}{\beta}$, then

$$f_Y(y) = \frac{1}{\beta} \exp\left[-e^{-g} - g\right], \tag{3.2}$$

where

$$g = g(y) = \frac{\alpha - y}{\beta}, \quad \alpha = \beta \ln(2\sigma^2) + b, \quad \beta = \frac{a}{2}.$$

The mean and variance of this distribution are

$$E(Y) = \overline{Y} = \alpha - \gamma\beta = \beta \left[\ln(2\sigma^2) - \gamma\right] + b$$

and

$$\text{var}(Y) = E\left[(Y - \overline{Y})^2\right] = \frac{(\pi\beta)^2}{6}, \tag{3.3}$$

where γ is the Euler constant, $\gamma \approx 0.5772$.

Remark: In the Rayleigh model, we assume that

$$\sigma = \frac{u}{\sqrt{2}},$$

where u denotes the pixel brightness of the noise-free image. Now if v is the pixel brightness of a compressed (noise-free) image, then $v = h(u)$ gives us that

$$u = h^{-1}(v) = \exp\left[\frac{v - b}{a}\right]$$

and hence

$$\sigma = \frac{u}{\sqrt{2}} = \frac{\exp\left[\frac{v-b}{a}\right]}{\sqrt{2}} = \exp\left[\frac{v - b}{a} - \frac{1}{2}\ln 2\right]. \tag{3.4}$$

Furthermore,

$$\alpha = \beta \ln(2\sigma^2) + b = \frac{a}{2} \ln(u^2) + b = a \ln u + b, \quad (b \geq 0).$$

3.2   Modeling of a Log-Compressed Image

Let f denote the intensity of a pixel, after having converted the Rayleigh-distributed ultrasound envelope to an electric signal. Thus, $0 \leq f < \infty$. We then apply the transformation (3.1) to log-compress the intensity to $h = a \ln f + b$.

Assumption: The values of a and b are chosen appropriately, and the signal is being clipped (either before or after compression) so that

$$0 \leq h \leq M$$

for some positive constant M (for example, $0 \leq h \leq 255$ when displayed as a BMP image). This assumption will slightly modify the PDF (3.2), but we assume that the clipping takes place at far ends of the PDF, so that the PDF (3.2) remains practically unchanged by this clipping.

3.3 The Proposed Model

We are now ready to present our proposed model for the removal of ultrasound speckle noise. We will employ the following model, assuming that the ultrasound image is log-compressed: the brightness or intensity of a pixel in the compressed noisy ultrasound image is a Fisher-Tippett random variable and thus has density function (3.2),

$$p_\sigma(r) = \frac{1}{\beta} e^{-\exp\left[\frac{r-\alpha}{\beta}\right] + \frac{r-\alpha}{\beta}}, \tag{3.5}$$

where σ is the parameter coming from the Rayleigh PDF and may vary from pixel to pixel. Note that the shifts a and b are identical for all pixels. The variance of p_σ is a measure of noise, and since by (3.3), the variance is

$$\frac{(\pi\beta)^2}{6},$$

i.e. it is independent of the parameter σ, we may consider this as additive noise.

To begin, we assume that the image takes the form of a square Ω of size $N \times N$. This is not really a restriction, as any image of square shape can be scaled to this size. The values $v_0(x, y)$, $f(x, y)$ and $v(x, y)$ represent the intensities of the unknown noiseless image, the given noisy image and the desired denoised image, respectively, at location (x, y), and may also be denoted by subscripts, for example $f_{x,y}$ instead of $f(x, y)$. Thus, these functions all take on positive values only on Ω. The noiseless image v_0 is unknown, the noisy image f is being measured, while the denoised image v to be found should be a good approximation to v_0.

Throughout, we will switch freely between this continuous and a discrete model: In the discrete model, the image is pixellated as

$$\Omega = \{(x, y) : x, y = 0, \ldots, N-1\},$$

so that $v_0(x, y)$, $f(x, y)$ and $v(x, y)$ represent the image intensities at pixel (x, y). When there is a large number of pixels of very small size each, after rescaling Ω to its original size, the discrete model can be considered a good approximation to the continuous model.

We let $\mathcal{X}$ denote the space of all possible images. Thus, elements of $\mathcal{X}$ are functions $v : \Omega \to (0, \infty)$. This is a probability space with an unknown probability measure. We wish to determine the image $v \in \mathcal{X}$ which is the most likely given an observed (noisy) image $f \in \mathcal{X}$. From the probabilistic point of view, the noiseless image and the noisy image are random variables V and F on $\mathcal{X}$, respectively, and we are going to find an image v to which V is the most likely, given the observed noisy image f. That is, we must find v which maximizes

$$P(V = v | F = f).$$

This image v will then be considered as the denoised image. The distributions of V and F will be discussed below. It turns out that the distribution of F is known at the pixel level only, thus we now proceed to consider each pixel individually.

Given any random variable U on $\mathcal{X}$, $U_{x,y}$ will denote the corresponding random variable of pixel intensity at pixel (x, y). Thus, $V_{x,y}$ is a random variable on $\mathbb{R}$. Here we make an important assumption: We assume that the image intensities $V_{x,y}$ (and similarly the image intensities $F_{x,y}$) at different pixels are independent. Thus,

$$P(V = v | F = f) = \prod_{(x,y) \in \Omega} P(V_{x,y} = v_{x,y} | F_{x,y} = f_{x,y}),$$

where $v_{x,y} = v(x, y)$ and $f_{x,y} = f(x, y)$. *Bayes' Rule* says that

$$P(V_{x,y} = v_{x,y} | F_{x,y} = f_{x,y}) = \frac{P(F_{x,y} = f_{x,y} | V_{x,y} = v_{x,y}) P(V_{x,y} = v_{x,y})}{P(F_{x,y} = f_{x,y})},$$

hence we need to maximize

$$\frac{\prod_{(x,y) \in \Omega} P(F_{x,y} = f_{x,y} | V_{x,y} = v_{x,y}) P(V_{x,y} = v_{x,y})}{\prod_{(x,y) \in \Omega} P(F_{x,y} = f_{x,y})}.$$

Since the denominator does not depend on v it suffices to maximize

$$\prod_{(x,y) \in \Omega} P(F_{x,y} = f_{x,y} | V_{x,y} = v_{x,y}) P(V_{x,y} = v_{x,y}). \tag{3.6}$$

Now by assumption, each $F_{x,y}$ is a Fisher-Tippett random variable with probability density

$$P(F_{x,y} = f_{x,y}) = p_\sigma(f_{x,y}) = \frac{1}{\beta} e^{-\exp\left[\frac{f_{x,y}-\alpha}{\beta}\right] + \frac{f_{x,y}-\alpha}{\beta}},$$

where as outlined in (3.4),

$$\sigma = \sigma(x,y) = \exp\left[\frac{v(x,y)-b}{a} - \frac{1}{2}\ln 2\right] = \exp\left[\frac{v_{x,y}-b}{a} - \frac{1}{2}\ln 2\right]$$

and

$$\alpha = \beta \ln(2\sigma^2) + b = \beta\left[2\frac{v_{x,y}-b}{a}\right] + b = v_{xy}.$$

Then

$$P(F_{x,y} = f_{x,y}|V_{x,y} = v_{x,y}) = p_\sigma(f_{x,y}) = \frac{1}{\beta} e^{-\exp\left[\frac{f_{x,y}-v_{x,y}}{\beta}\right] + \frac{f_{x,y}-v_{x,y}}{\beta}}.$$

Expression (3.6) becomes

$$\left(\prod_{(x,y)\in\Omega} \frac{1}{\beta} e^{-\exp\left[\frac{f_{x,y}-v_{x,y}}{\beta}\right] + \frac{f_{x,y}-v_{x,y}}{\beta}}\right) \left(\prod_{(x,y)\in\Omega} P(V_{x,y} = v_{x,y})\right)$$

that is,

$$\left(\prod_{(x,y)\in\Omega} \frac{1}{\beta} e^{-\exp\left[\frac{f_{x,y}-v_{x,y}}{\beta}\right] + \frac{f_{x,y}-v_{x,y}}{\beta}}\right) P(V = v). \tag{3.7}$$

Since the function $-\ln$ is decreasing and β is constant, maximizing (3.7) is equivalent to minimizing

$$-\ln[P(V = v)] + \sum_{(x,y)\in\Omega} \left(\exp\left[\frac{f_{x,y}-v_{x,y}}{\beta}\right] - \frac{f_{x,y}-v_{x,y}}{\beta}\right).$$

We regard this as a discrete approximation of the functional

$$E(v) = -\ln\Phi(v) + \int_\Omega \left(\exp\left[\frac{f-v}{\beta}\right] - \frac{f-v}{\beta}\right),$$

where $\Phi(v)$ is the density function of the random variable V.

Now Green (2002) has shown that for the model of a variational approach, this density function is

$$\Phi(v) = e^{-\lambda \int_\Omega |\nabla v|},$$

where λ is a positive parameter. Hence, the functional $E(v)$ becomes

$$E(v) = \lambda \int_\Omega |\nabla v| + \int_\Omega \left(\exp\left[\frac{f-v}{\beta}\right] - \frac{f-v}{\beta}\right).$$

Since f is independent of v, it suffices to minimize the functional

$$E(v) = \int_\Omega |\nabla v| + \frac{1}{\lambda} \int_\Omega \left(e^{f/\beta} e^{-v/\beta} + \frac{v}{\beta} \right). \tag{3.8}$$

The formal Euler-Lagrange equation for minimizing $E(v)$ is then

$$\text{div} \left(\frac{\nabla v}{|\nabla v|} \right) + \frac{1}{\lambda\beta} \left(e^{f/\beta} e^{-v/\beta} - 1 \right) = 0, \tag{3.9}$$

where $\beta = \dfrac{a}{2}$. That is,

$$\frac{\partial}{\partial x} \frac{v_x}{\sqrt{v_x^2 + v_y^2}} + \frac{\partial}{\partial y} \frac{v_y}{\sqrt{v_x^2 + v_y^2}} + \frac{1}{\lambda\beta} \left(e^{f/\beta} e^{-v/\beta} - 1 \right) = 0. \tag{3.10}$$

3.4 Numerical Treatment of the Model

This section presents the numerical scheme used in this thesis. We consider the solution of the Euler-Lagrange equation (3.10) as the steady-state solution of a parabolic partial differential equation.

$$v_t = \frac{\partial}{\partial x} \left(\frac{v_x}{\sqrt{v_x^2 + v_y^2}} \right) + \frac{\partial}{\partial y} \left(\frac{v_y}{\sqrt{v_x^2 + v_y^2}} \right) + \frac{1}{\lambda\beta} \left(e^{(f-v)/\beta} - 1 \right), \tag{3.11}$$

with initial condition $v(x, y, 0) = f(x, y)$ on Ω and the boundary condition $v(x, y, t) = f(x, y)$ on the boundary $\partial\Omega$ of the square Ω. In order to solve problem (3.11) numerically, the images are again pixellated, so that the spatial domain space is considered as an $N \times N$ square grid. The grid point (i, j) corresponds to location (x_i, y_j), $i = 0 \ldots N - 1, j = 0 \ldots N - 1$, where $x_i = ih$, $y_j = jh$ and $Nh = 1$.

Denote $v_{ij}^n = v(x_i, y_j, t_n)$ where $t_n = n\Delta t$, $n = 0, 1, 2, \ldots$ and Δt is step size, and set $v_{ij}^0 = f_{ij}$, Following Rudin et al. (1992), the numerical scheme of problem (3.11) is

$$
\begin{aligned}
v_{ij}^{n+1} &= v_{ij}^n + \frac{\Delta t}{h} \left[\Delta_-^x \left(\frac{\Delta_+^x v_{ij}^n}{\sqrt{(\Delta_+^x v_{ij}^n)^2 + (m(\Delta_+^y v_{ij}^n, \Delta_-^y v_{ij}^n))^2}} \right) \right] \\
&\quad + \frac{\Delta t}{h} \left[\Delta_-^y \left(\frac{\Delta_+^y v_{ij}^n}{\sqrt{(\Delta_+^y v_{ij}^n)^2 + (m(\Delta_+^x v_{ij}^n, \Delta_-^x v_{ij}^n))^2}} \right) \right] \\
&\quad + \frac{\Delta t}{\lambda\beta} \left(e^{(f_{ij} - v_{ij}^n)/\beta} - 1 \right),
\end{aligned}
\tag{3.12}
$$

with boundary conditions

$$v_{0j}^n = f_{0j}$$

$$v_{(N-1)j}^n = f_{(N-1)j}$$

$$v_{i0}^n = f_{i0}$$

$$v_{i(N-1)}^n = f_{i(N-1)}$$

where $\Delta_{\pm}^x \Theta_{ij} = \pm(\Theta_{(i\pm1)j} - \Theta_{ij})$ and similarly for $\Delta_{\pm}^y \Theta_{ij}$. The step size Δt and h are chosen for stability such that

$$\frac{\Delta t}{h} \leq 1.$$

Here,

$$m(a,b) = \frac{\text{sgn}(a) + \text{sgn}(b)}{2} \min(|a|, |b|).$$

where

$$\text{sgn}(x) = \begin{cases} -1 & \text{if } x < 0, \\ 0 & \text{if } x = 0, \\ 1 & \text{if } x > 0. \end{cases}$$

Note that if v_{ij}^n converges as $n \to \infty$, then $\dfrac{v_{ij}^{n+1} - v_{ij}^n}{\Delta t} \to 0$ as $n \to \infty$. Thus, the numerical solution of problem (3.12) will converge to an approximate solution of the equation

$$\frac{\partial}{\partial x}\left(\frac{v_x}{\sqrt{v_x^2 + v_y^2}}\right) + \frac{\partial}{\partial y}\left(\frac{v_y}{\sqrt{v_x^2 + v_y^2}}\right) + \frac{1}{\lambda\beta}\left(e^{(f-v)/\beta} - 1\right) = 0,$$

where $v = f$ on $\partial\Omega$, which is the denoised image of our model.

CHAPTER IV

RESULTS AND DISCUSSION

This chapter presents results from images with noise overlay and images after noise reduction. The image quality evaluations include Absolute Difference (AD), Root Mean Square Error (RMSE), Correlation Coefficient (Corr), and Universal Quality Index (UQI). However, this chapter presents only a selection of results that show significant differences in quality. Most of the evaluation results are provided in Appendix B. For each evaluation:

- Absolute Difference (AD) – lower values indicate better quality.

- Root Mean Square Error (RMSE) – lower values indicate better quality.

- Correlation Coefficient (Corr) – higher values indicate better quality.

- Universal Quality Index (UQI) – higher values indicate better quality.

4.1   Lena Image and Noisy Lena Image

The image used in this thesis to test our proposed method is the Lena image. The Lena image (also known as Lenna) is one of the most famous test images in the field of image processing and computer vision. It is a 512×512 pixel grayscale image of a woman, cropped from a 1972 issue of Playboy magazine. The Lena image is shown in Figure 4.1.

Starting from the original grayscale image, pixel intensities are transformed using an exponential function to create a signal representation. Next, Rayleigh-distributed noise is then added to simulate real-world distortions. Next, a logarithmic transformation is applied to convert the noisy signal back into an image intensity format. During this process, the resulting noisy image is normalized to maintain a valid intensity range. In the final step, the average intensity of the noisy image is adjusted to match that of the original image. The resulting noisy Lena image is shown in Figure 4.2.
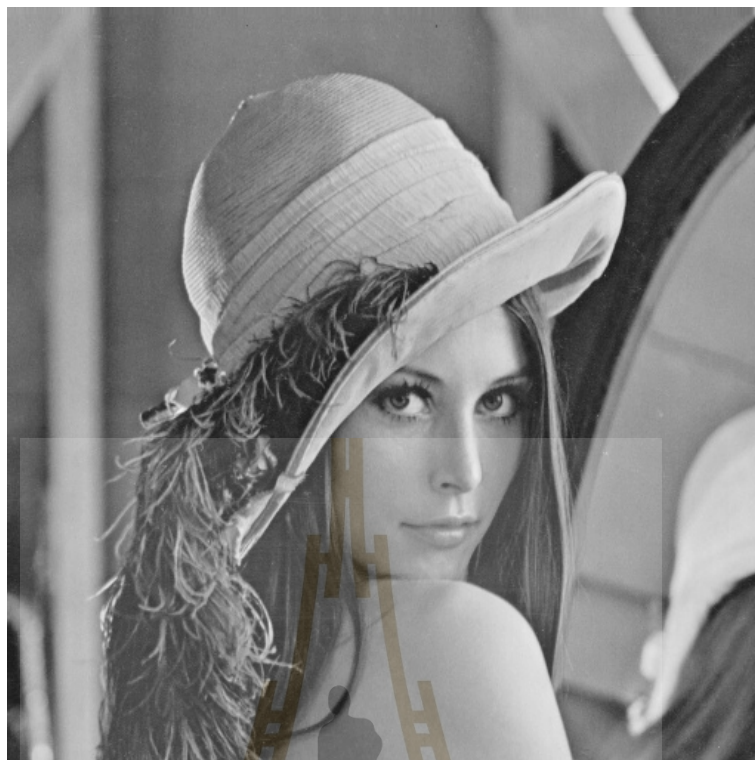
Figure 4.1 Lena Image.

Figure 4.2 Lena Image Overlaid with Gumbel Noise.

4.2   Images for Different Beta Values

This section evaluates the performance of image noise reduction with the proposed method using various parameters.

4.2.1   Images for β = 0.1

(a) $\beta = 0.1, \lambda = 3.00$ (b) $\beta = 0.1, \lambda = 4.00$ (c) $\beta = 0.1, \lambda = 5.00$

(d) $\beta = 0.1, \lambda = 6.00$ (e) $\beta = 0.1, \lambda = 7.00$ (f) $\beta = 0.1, \lambda = 8.00$

Figure 4.3 Images for β = 0.1.

Table 4.1 Table of evaluation images for different λ values for β=0.1.

Image	λ	AD	RMSE	Corr	UQI
(a)	3.00	0.047	0.217	0.962	0.956
(b)	4.00	0.044	0.210	0.975	0.966
(c)	**5.00** (joint best)	**0.044**	**0.210**	**0.979**	**0.968**
(d)	**6.00** (joint best)	**0.044**	**0.211**	**0.980**	**0.968**
(e)	7.00	0.045	0.212	0.980	0.967
(f)	8.00	0.045	0.214	0.979	0.966

4.2.2 Images for β = 0.2

(a) $\beta = 0.2, \lambda = 0.10$

(b) $\beta = 0.2, \lambda = 0.50$

(c) $\beta = 0.2, \lambda = 1.00$

(d) $\beta = 0.2, \lambda = 1.65$

(e) $\beta = 0.2, \lambda = 2.50$

(f) $\beta = 0.2, \lambda = 4.00$

Figure 4.4 Images for β = 0.2.

Table 4.2 Table of evaluation images for different λ values for β=0.2.

Image	λ	AD	RMSE	Corr	UQI
(a)	0.10	0.186	0.282	0.854	0.854
(b)	0.50	0.061	0.248	0.906	0.905
(c)	1.00	0.041	0.203	0.967	0.960
(d)	**1.65** (Best)	**0.037**	**0.193**	**0.980**	**0.969**
(e)	2.50	0.039	0.197	0.978	0.965
(f)	4.00	0.041	0.204	0.973	0.957

4.2.3 Images for β = 0.3

(a) $\beta = 0.1, \lambda = 0.10$ (b) $\beta = 0.3, \lambda = 0.30$ (c) $\beta = 0.3, \lambda = 0.50$

(d) $\beta = 0.3, \lambda = 0.75$ (e) $\beta = 0.3, \lambda = 1.25$ (f) $\beta = 0.3, \lambda = 2.00$

Figure 4.5 Images for β = 0.3.

Table 4.3 Table of evaluation images for different λ values for β=0.3.

Image	λ	AD	RMSE	Corr	UQI
(a)	0.10	0.080	0.282	0.854	0.854
(b)	0.30	0.053	0.230	0.929	0.926
(c)	0.50	0.039	0.198	0.969	0.961
(d)	**0.75** (Best)	**0.036**	**0.189**	**0.979**	**0.969**
(e)	1.25	0.038	0.194	0.977	0.963
(f)	2.00	0.041	0.202	0.971	0.955

4.2.4   Images for β = 0.5

(a) $\beta = 0.5, \lambda = 0.05$ (b) $\beta = 0.5, \lambda = 0.15$ (c) $\beta = 0.5, \lambda = 0.25$

(d) $\beta = 0.5, \lambda = 0.30$ (e) $\beta = 0.5, \lambda = 0.75$ (f) $\beta = 0.5, \lambda = 1.50$

Figure 4.6 Images for β = 0.5.

Table 4.4 Table of evaluation images for different λ values for β=0.5.

Image	λ	AD	RMSE	Corr	UQI
(a)	0.05	0.074	0.271	0.870	0.870
(b)	0.15	0.044	0.209	0.952	0.947
(c)	0.25	0.036	0.189	0.977	0.967
(d)	**0.30** (Best)	**0.036**	**0.188**	**0.978**	**0.967**
(e)	0.75	0.040	0.201	0.970	0.954
(f)	1.50	0.045	0.212	0.959	0.938

4.2.5 Images for β = 0.8

| (a) $\beta = 0.8, \lambda = 0.05$ | (b) $\beta = 0.8, \lambda = 0.10$ | (c) $\beta = 0.8, \lambda = 0.25$ |
| (d) $\beta = 0.8, \lambda = 0.50$ | (e) $\beta = 0.8, \lambda = 1.00$ | (f) $\beta = 0.8, \lambda = 2.00$ |

Figure 4.7 Images for β = 0.8.

Table 4.5 Table of evaluation images for different λ values for β=0.8.

Image	λ	AD	RMSE	Corr	UQI
(a)	0.05	0.048	0.219	0.939	0.935
(b)	**0.10** (Best)	**0.036**	**0.189**	**0.976**	**0.965**
(c)	0.25	0.039	0.198	0.972	0.957
(d)	0.50	0.044	0.210	0.961	0.942
(e)	1.00	0.048	0.218	0.949	0.926
(f)	2.00	0.049	0.222	0.942	0.917

4.2.6   Images for β = 1.0

(a) $\beta = 1.0, \lambda = 0.05$ (b) $\beta = 1.0, \lambda = 0.10$ (c) $\beta = 1.0, \lambda = 0.25$

(d) $\beta = 1.0, \lambda = 0.50$ (e) $\beta = 1.0, \lambda = 1.00$ (f) $\beta = 1.0, \lambda = 2.00$

Figure 4.8 Images for $\beta = 1.0$.

Table 4.6 Table of evaluation images for different λ values for $\beta = 1.0$.

Image	λ	AD	RMSE	Corr	UQI
(a)	0.05	0.038	0.196	0.967	0.959
(b)	**0.10** (Best)	**0.037**	**0.191**	**0.977**	**0.964**
(c)	0.25	0.042	0.206	0.966	0.948
(d)	0.50	0.047	0.216	0.953	0.931
(e)	1.00	0.049	0.221	0.944	0.919
(f)	2.00	0.050	0.224	0.941	0.914

4.2.7　Best Performance Noise Reduction for Each β

Based on the previous section, this section presents the cases with the highest noise reduction efficiency for β values of 0.1, 0.2, 0.3, 0.5, 0.8, and 1.0.

| (a) $\beta = 0.1, \lambda = 5.00$ | (b) $\beta = 0.2, \lambda = 1.65$ | (c) $\beta = 0.3, \lambda = 0.75$ |
| (d) $\beta = 0.5, \lambda = 0.30$ | (e) $\beta = 0.8, \lambda = 0.10$ | (f) $\beta = 1.0, \lambda = 0.10$ |

Figure 4.9 Images for each β.

Table 4.7 Performance Evaluation of the Best Values for Each β.

Image	β	λ	AD	RMSE	Corr	UQI
(a)	0.1	5.00	0.044	0.210	0.979	0.968
(b)	0.2	1.65	0.037	0.193	0.980	0.969
(c)	**0.3**	**0.75**	**0.036**	**0.189**	**0.979**	**0.969**
(d)	0.5	0.30	0.036	0.188	0.978	0.967
(e)	0.8	0.10	0.036	0.189	0.976	0.965
(f)	1.0	0.10	0.037	0.191	0.977	0.964

CHAPTER V

CONCLUSION

In this thesis, a novel approach for medical ultrasound image enhancement was proposed using the Gumbel distribution to effectively reduce speckle noise while preserving important anatomical details. Speckle noise is a common issue in ultrasound imaging, often reducing image clarity and making medical diagnoses more challenging. To address this, a mathematical model based on calculus of variations was developed, allowing for an optimized noise reduction framework that balances image denoising with structural preservation.

Through extensive evaluation, the proposed model was tested on various ultrasound images with different parameter settings. The performance was assessed using key quality metrics: Absolute Difference (AD), Root Mean Square Error (RMSE), Correlation Coefficient (Corr), and Universal Quality Index (UQI). Among the different configurations, the combination of $\beta = 0.3$ and $\lambda = 0.75$ yielded the most promising results, as it demonstrated the lowest AD (0.036), very low RMSE (0.189), very high Corr (0.980) and the highest UQI values (0.969). This finding indicates that the selected parameters achieve an optimal balance between noise reduction and detail retention, making it the most effective choice for enhancing ultrasound images.

The significance of this work lies in its ability to provide a mathematically grounded and computationally efficient method for ultrasound image enhancement. Unlike deep learning-based approaches, which often function as black-box models, this method offers a clear, interpretable, and adaptable framework that can be fine-tuned for different imaging conditions. Furthermore, the use of the Gumbel distribution introduces a new perspective on modeling noise in medical imaging, opening the door for future research in statistical image processing.
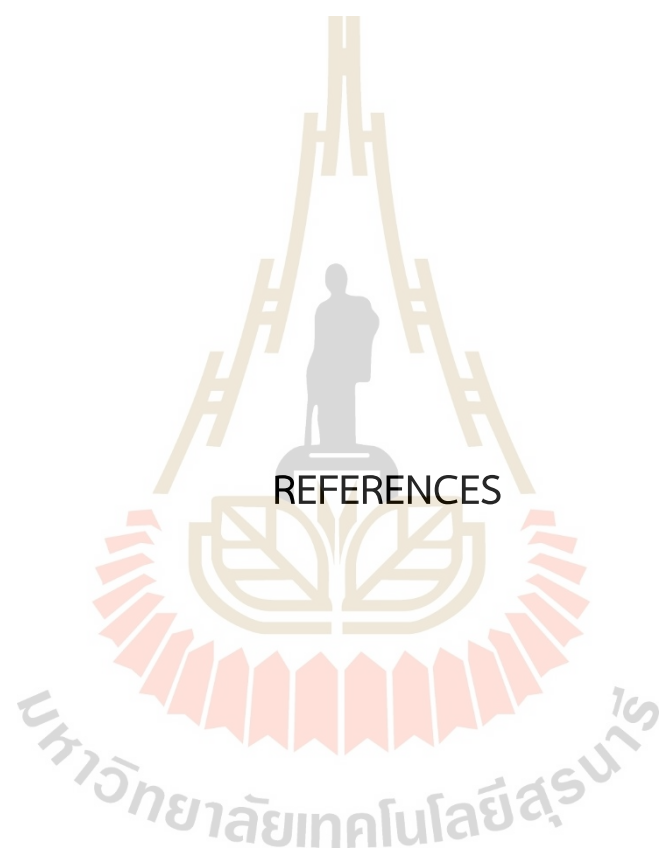
REFERENCES

REFERENCES

Almutiry, W., Alahmadi, A. A., Elbatal, I., Ragab, I. E., Balogun, O. S., and Elgarhy, M. (2021). Application to engineering and medical data using three-parameter exponential model. *Mobile Information Systems, 2021*, Article ID 9550156, 1–14. `https://doi.org/10.1155/2021/9550156`

Ateeq, K., Qasim, T. B., and Alvi, A. R. (2019). An extension of Rayleigh distribution and applications. *Cogent Mathematics & Statistics, 6*(1), Article ID 1622191. `https://doi.org/10.1080/25742558.2019.1622191`

Bakouch, H. S., Hussain, T., Tošić, M., Stojanović, V. S., and Qarmalah, N. (2023). Unit exponential probability distribution: Characterization and applications in environmental and engineering data modeling. *Mathematics, 11*(4207). `https://doi.org/10.3390/math11194207`

Bashir, S., and Rasul, M. (2018). A new weighted Rayleigh distribution: Properties and applications on lifetime data. *Open Journal of Statistics, 8*(3), 640–650. `https://doi.org/10.4236/ojs.2018.83041`

Booth, B., and Li, X. (2007). Boundary point detection for ultrasound image segmentation using Gumbel distributions. In *Proceedings of the Second International Conference on Signal Processing and Multimedia Applications* (pp. 175–179). SciTePress. `https://doi.org/10.5220/0002138701750179`

Gonzalez, C. R., and Woods, R. (2018). *Digital Image Processing*. (4th ed.). Pearson.

Green, M. L. (2002). Statistics of images, the TV algorithm of Rudin-Osher-Fatemi for image denoising, and an improved denoising algorithm. Department of Mathematics and Institute for Pure and Applied Mathematics, UCLA.

Hashim, F. A., Hussien, A. G., Bouaouda, A., Samee, N. A., Khurma, R. A., Alamro, H., and Al-Betar, M. A. (2024). An enhanced exponential distribution optimizer and its appli-

cation for multi-level medical image thresholding problems. *Alexandria Engineering Journal, 93,* 142–188. `https://doi.org/10.1016/j.aej.2024.02.012`

Krishnamoorthy, K. (2006). *Handbook of Statistical Distributions with Applications*. Chapman & Hall/CRC.

Mahmoud, M. A. W., Kilany, N. M., and El-Refai, L. H. (2020). The power Rayleigh distribution with an application on hydrological data. *Journal of Statistical and Applied Mathematical Sciences,* 8(2), 123–137. `https://doi.org/10.22541/au.158714136.67784006`

Mansouri, N. J., Khaissidi, G., Despaux, G., Mrabti, M., and Le Clezio, E. (2022). Ultrasonic signal noise reduction based on convolutional autoencoders for NDT applications. *E3S Web of Conferences, 351,* 01039. Innovation and Modern Applied Science in Environmental Studies 2022 (ICIES'22). `https://doi.org/10.1051/e3sconf/202235101039`

NIST/SEMATECH. (2012). *NIST/SEMATECH e-Handbook of Statistical Methods*. National Institute of Standards and Technology. `https://doi.org/10.18434/M32189`

Read, C. B., Balakrishnan, N., Vidakovic, B., and Kotz, S. (2005). *Encyclopedia of statistical sciences* (2nd ed.). Wiley-Interscience. `https://1lib.sk/book/505575/466990/encyclopedia-of-statistical-sciences.html`

Rudin, L. I., Osher, S., and Fatemi, E. (1992). Nonlinear total variation based noise removal algorithms. *Physica D: Nonlinear Phenomena, 60,* 259-268. `https://api.semanticscholar.org/CorpusID:13133466`

Seekot, W. (2008). Ultrasound image enhancement by means of a variational approach (Master's thesis). Suranaree University of Technology, Nakhon Ratchasima, Thailand.

Shrivastava, A., Shinde, M., and Lawande, P. P. (2007). An approach-effect of an exponential distribution on different medical images. *IJCSNS International Journal of Computer Science and Network Security, 7*(9), 235–241. `https://api.semanticscholar.org/CorpusID:55454326`

Takagi, R. and Koseki, Y. (2022). Noise reduction technique using deep learning for ultra-sound imaging during high intensity focused ultrasound treatment. *Japanese Journal of Applied Physics. 61*. `10.35848/1347-4065/ac5292.`

Tanthanuch, J., Seekot, W., and Schulz, E. (2012). Ultrasound image enhancement by means of a variational approach. In *Proceedings of the 12th AOCMP & 10th SEACOMP Conference* (pp. 323–326). Chiang Mai, Thailand.

Tanthanuch, J., and Schulz, E. (2015). Analysis of noise reduction in medical ultrasound imaging (Research Report No. SUT1-103-54-12-27). Suranaree University of Technology, Nakhon Ratchasima, Thailand.

Zhou, Wang, Alan, C., and Bovik. (2002). A universal image quality index. *IEEE Signal Processing Letters, 9*(3): 81-84. `doi:10.1109/97.995823`
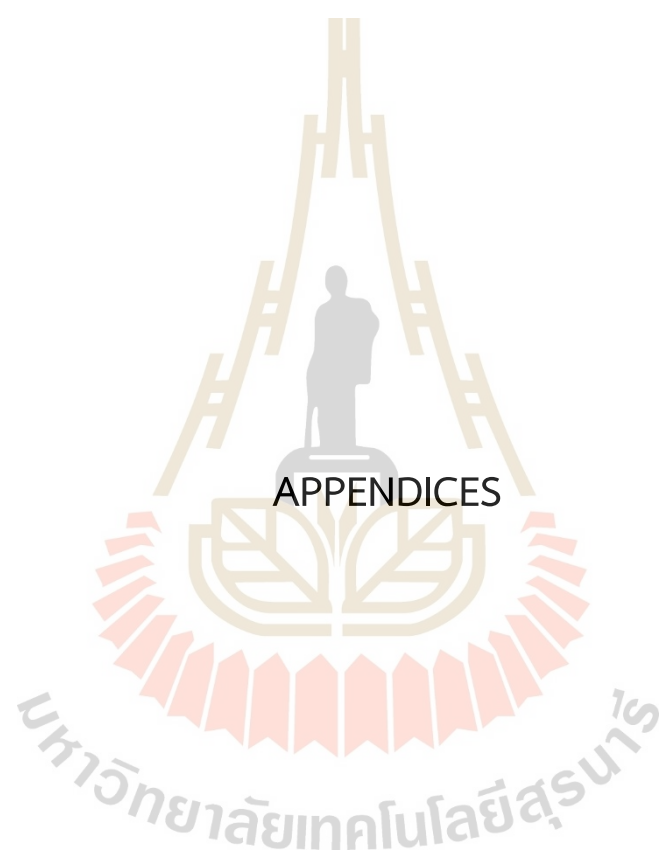
APPENDICES

APPENDIX A

APPLICATION OF PYTHON CODE IN IMAGE NOISE

OVERLAYING AND IMAGE NOISE REDUCTION

This chapter presents some Python code using in this thesis.

A.1   The Image Noise Overlaying Python Code

The presented Python script introduces Gumbel noise to an image and modifies its intensity using an exponential transformation. The goal is to simulate a noisy image while maintaining a similar average intensity to the original image.

Key Steps in the Process:

1. Read the original grayscale image and normalize its intensity.

2. Convert pixel intensities using an exponential function to create a signal representation.

3. Add Rayleigh-distributed noise to simulate real-world distortions.

4. Apply logarithmic transformation to convert the noisy signal back into an image intensity format.

5. Normalize the resulting noisy image to maintain a valid intensity range.

6. Adjust the noisy image's average intensity to match that of the original image.

7. Display the original, noisy, and adjusted images for visual comparison.

```
1   """
2   This code adds Gumbel noise to an image
3
4   """
5
6   import cv2
7   import numpy as np
8   from matplotlib import pyplot as plt
9   import math
10  from scipy.stats import gumbel_r
11  #import sys
12
```

```
13
14  #### specify directories and file names ##################################
15
16  outfiledir = "."
17
18  image_name = "lena"
19  orig_image_name       =  'lena512.bmp'                     # noiseless image
20  noisy_image_name      =  'lena512_noise_rayleigh_new.bmp'
21  wb2_noisy_image_name    =   'lena512_noise_wb2_new.bmp'
22
23  #############################################################################
24
25  ##     read as greyscale (pixel brightness:    0..1)
26  orig_img = cv2.imread(orig_image_name,cv2.IMREAD_GRAYSCALE)
27  ## display noiseless image on screen
28
29  m,n =  orig_img.shape                    # image size m x n  pixels
30  mm = np.mean(orig_img)
31  #print(mm)
32  norm_img = orig_img /255*math.log(255)
33  new_img = norm_img*1                  # prepare array for the new image
34  for i in range(m):
35      for j in range(n):
36          x = math.exp(norm_img[i][j])/math.sqrt(2)
37          ###### convert image to signal in exponential from #############
38          v = np.random.rayleigh( scale = x )
39          ###### v is the Rayleigh noise from the signal #################
40          lv = math.log(v)
41          ###### lv is the intensity of the image from the signal #########
42          if lv>=0:
43              new_img[i][j] = lv
44          else:
45              new_img[i][j] = 0
46
47  new_img = new_img-np.min(new_img)
48  new_img = new_img*255/np.max(new_img)
```

```
49
50   plt.imshow(orig_img, cmap='gray')  ;  plt.title('Original Image') ; plt.show()
51   plt.imshow(new_img, cmap='gray')  ;  plt.title('Exponented Image') ; plt.show()
52
53   ########## Display the original and the noisy images ######################
54   noise = orig_img-new_img3
55   ########## Find the noise of the image ###############################
56
57   #This part want to change the noisy images the have the same average intensity with
58   # the original image
59   mean1 = np.mean(orig_img)
60   mean2 = np.mean(new_img)
61    diff = mean1-mean2
62   new_img2 = new_img+diff
63   plt.imshow(new_img2, cmap='gray')  ;  plt.title('Exponented Image 2') ; plt.show()
```
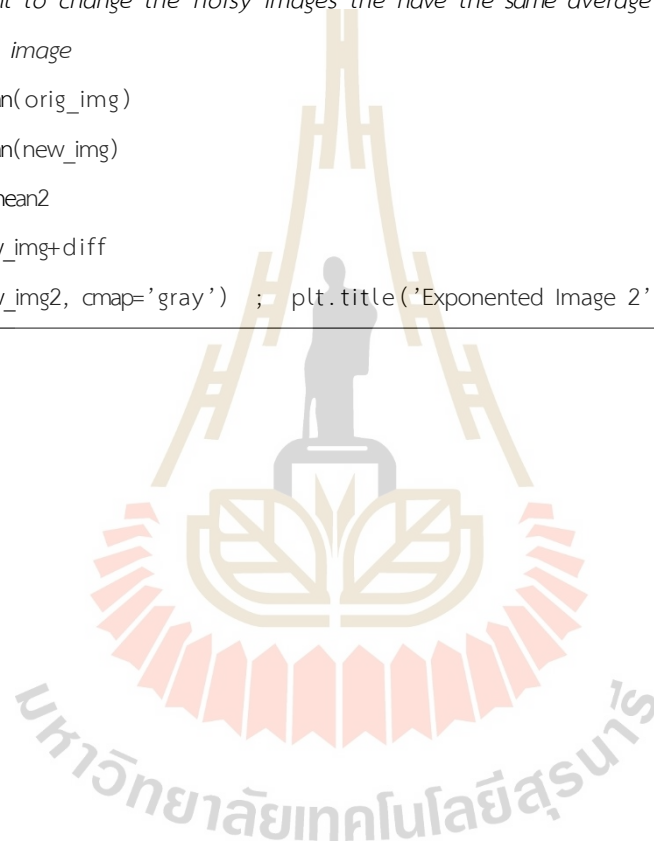
A.2 The Image Noise Reduction Python Code

The proposed Python script implements and evaluates three variational image denoising methods:

1. Gumbel-noise Model

2. Le et al. Model

3. ROF (Rudin-Osher-Fatemi) Model

The script denoises an image corrupted by noise using these models while varying the β parameter, which controls the balance between noise removal and image fidelity. The Partial Differential Equation (PDE) approach is used for solving the denoising problem iteratively.

Key points of the implementation:

- The program reads an original and a noisy grayscale image.

- Users can select a denoising model.

- The PDE solver refines the image using gradient-based updates.

- Various image quality metrics are computed, including:

    - Absolute Difference (AD) – lower is better.

    - Root Mean Square Error (RMSE) – lower is better.

    - Correlation Coefficient (Corr) – higher is better.

    - Universal Quality Index (UQI) – higher is better.

- The script saves the denoised images for various β values and displays them.

Overall, this script effectively compares different variational denoising techniques, allowing users to analyze their performance based on computed metrics.

```
1  """
2  This code implements several variational methods for image denoising:
3
4     1. our model (Gumbel-noise)
5     2. Le et al.  model
6     3. ROF model
7
8  a)  All models contain a parameter 'beta' giving weight to the data fidelity term.
9      This code denoises for a range of this parameter, from
10     beta=beta_min    to    beta=beta_max    in stepsize  beta_step
11
12 b) Metrics that match the denosed image with the noiseless image are:
13     AD  (L1-norm) -- lower is better
14     RMSE (L2-norm) -- lower is better
15     Corr  (Correlation Coefficient) -- higher is better
16     UQI  (UQI Universal quality index) -- higher is better
17
18 """
19
20 import cv2
21 from matplotlib import pyplot as plt
22 import numpy as np
23 import sys
24 import time
25
26 #### specify directories and file names ##################################
27
28 outfiledir = "images"
29
30 image_name = "lena"
31 orig_image_name       =  'lena512.bmp'
32 noisy_image_name      =  'lena512_noise_rayleigh_.bmp'
33
34 ##### specify parameters ############################
35
```

```
36   beta_min = 0.2

37   beta_max = 8.0

38   beta_step = 0.2

39   #

40   #   parameters for solving PDE

41   #

42   Delta_t=0.01   # time stepsizes for PDE

43   hh=1           #

44   N=1000         # number of time steps

45

46   np.seterr( all= 'raise' )                ### catch any floating point error

47

48   #################################################

49   #   start the code

50   #################################################

51

52   ##     read as greyscale

53   noisy_img    = cv2.imread(noisy_image_name, 0 ).astype(float)/255

54   orig_img     = cv2.imread(orig_image_name, 0 ).astype(float)/255

55

56   if  noisy_img.shape != orig_img.shape:

57       sys.exit("*** Error:  original and noise images are of different sizes")

58

59

60   m,n =  noisy_img.shape              # image size mxn

61

62   step = Delta_t/hh;

63   fsquare = np.multiply( noisy_img , noisy_img  )

64

65

66   ## setup those parameters for image display which are independent of beta-loop.

67   ## normally these come AFTER computations

68

69   choice = input("enter data fidelity term: 1=Rayleigh,  2=Le et al.,  3=ROF : ")

70

71   match choice:
```

```
72          case '1':            # 1.  our method
73             method = "_Rayleigh variational_";
74          case '2':            # 2.  Le et al. method
75             method="_Le variational_";
76          case _:              # 3.  ROF method
77             method="_ROF variational_";
78
79   plt.imshow(orig_img, cmap='gray')  ;  plt.title('Original Image') ; plt.show()
80   plt.imshow(noisy_img, cmap='gray') ;  plt.title('Noisy Image') ; plt.show()
81
82
83   #w=1;           ### so that we can compare with other filters , we don't measure two rows of
          pixels along the border. Needed ?????
84   size_small     = (m-2) * (n-2);              ## size of image with border-pixels removed
85   orig_img_small  = orig_img[ 1:m-1, 1:m-1 ] ##  original image with border pixels removed
86   windowstext = str(m) + 'x' + str(n)
87
88
89   #
90   # loop over beta   0.1 ... 2.0  in 0.1 steps
91   #
92   beta = beta_min
93   while (beta <= beta_max ):
94      two_over_beta=2.0/beta;
95
96      ##  We solve the PDE using the .... method
97      ##
98      ##   begin with blank picture
99
100     u_old = np.ones( (m,n) )*0.5;                          ### initial values of u_old
          are 0.5
101     #
102     ###This is not free boundary !!!  We fix the boundary pixels Can we do this differently
          ?
103     #
104     u_old[0,:] = noisy_img[0,:];        u_old[m-1,:] = noisy_img[ m-1, : ]
```

```python
105     u_old[:,0] = noisy_img[:,0];         u_old[:,n-1] = noisy_img[ :  ,n-1]
106     u_new = u_old;                       ## allocate space
107
108     cur_time = time.time()
109     for k in range(N):
110         Delta_x_plus  = u_old[ 2:m, 1:n-1 ] - u_old[ 1:m-1, 1:n-1 ]   ### forward
                delta_u_x
111         Delta_x_minus = u_old[ 1:m-1, 1:n-1 ] - u_old[ 0:m-2, 1:n-1 ]   ### backward delta
                u_x
112         Min_Delta_x   = np.minimum(     np.abs( Delta_x_minus ), np.abs( Delta_x_plus )
                )
113         mx = np.multiply(  np.sign( Delta_x_plus ) + np.sign( Delta_x_minus ) , Min_Delta_x
                ) / 2.
114         #
115         Delta_y_plus  = u_old[ 1:m-1, 2:n ] - u_old[ 1:m-1, 1:n-1 ]   ### forward
                delta_u_y
116         Delta_y_minus = u_old[ 1:m-1, 1:n-1 ] - u_old[ 1:m-1, 0:n-2 ]   ### backward delta
                u_y
117         Min_Delta_y   = np.minimum(     np.abs( Delta_y_minus ), np.abs( Delta_y_plus )
                )
118         my = np.multiply(  np.sign( Delta_y_plus ) + np.sign( Delta_y_minus ) , Min_Delta_y
                ) / 2.
119         #
120         Delta_x_plus_bef_x  = u_old[ 1:m-1, 1:n-1 ] - u_old[ 0:m-2, 1:n-1 ]   ## check !
121         Delta_x_plus_bef_y  = u_old[ 2:m,   0:n-2 ] - u_old[ 1:m-1, 0:n-2 ]
122         Delta_x_minus_bef_y = u_old[ 1:m-1, 0:n-2 ] - u_old[ 0:m-2, 0:n-2 ]
123         Min_Delta_x_bef_y   = np.minimum(     np.abs( Delta_x_minus_bef_y ),  np.abs(
                Delta_x_plus_bef_y )    )
124         mx_bef_y = np.multiply(  np.sign( Delta_x_plus_bef_y ) + np.sign(
                Delta_x_minus_bef_y ) , Min_Delta_x_bef_y ) / 2.
125         #
126         Delta_y_plus_bef_y   = u_old[ 1:m-1, 1:n-1 ] - u_old[ 1:m-1, 0:n-2 ]
127         Delta_y_plus_bef_x   = u_old[ 0:m-2, 2:n   ] - u_old[ 0:m-2, 1:n-1 ]
128         Delta_y_minus_bef_x  = u_old[ 0:m-2, 1:n-1 ] - u_old[ 0:m-2, 0:n-2 ]
129         Min_Delta_y_bef_x    = np.minimum( np.abs( Delta_y_minus_bef_x ), np.abs(
                Delta_y_plus_bef_x )  )
```

```
130    my_bef_x = np.multiply(  np.sign( Delta_y_plus_bef_x ) + np.sign(
            Delta_y_minus_bef_x ) , Min_Delta_y_bef_x ) / 2.
131    #
132    # Avoid division by zero below
133    #
134    Divisor = np.sqrt(  np.square( Delta_x_plus ) + np.square( my )  )
135    Divisor = np.where(  np.abs( Divisor ) < 1e-10,  1.0, Divisor )        ## Avoid
            division by zero ==> instead, divide by 1
136    term_1  = np.divide( Delta_x_plus, Divisor )
137    #
138    Divisor = np.sqrt(  np.square( Delta_y_plus ) + np.square( mx )  )
139    Divisor = np.where(  np.abs( Divisor ) < 1e-10,  1.0, Divisor )        ## Avoid
            division by zero ==> instead, divide by 1
140    term_2  = np.divide( Delta_y_plus , Divisor )
141    #
142    Divisor = np.sqrt(  np.square( Delta_x_plus_bef_x ) + np.square( my_bef_x )  )
143    Divisor = np.where(  np.abs( Divisor ) < 1e-10,  1.0, Divisor )        ## Avoid
            division by zero ==> instead, divide by 1
144    term_1_bef_x = np.divide( Delta_x_plus_bef_x , Divisor )
145    #
146    Divisor = np.sqrt(  np.square( Delta_y_plus_bef_y ) + np.square( mx_bef_y )  )
147    Divisor = np.where(  np.abs( Divisor ) < 1e-10,  1.0, Divisor )        ## Avoid
            division by zero ==> instead, divide by 1
148    term_2_bef_y = np.divide( Delta_y_plus_bef_y , Divisor )
149    #
150    Delta_u_xx = term_1 - term_1_bef_x;
151    Delta_u_yy = term_2 - term_2_bef_y;
152    ###
153    u_new[ 1:m-1, 1:n-1 ] = u_old[ 1:m-1, 1:n-1 ] + step*( Delta_u_xx + Delta_u_yy );
154
155    match choice:
156        case '1':              ## 1.  our method
157            ### required for our method
158            u_old_square = np.square( u_old )
159            u_old_cube   = np.power( u_old, 3 )
160            u_old_cube[ abs(u_old_cube) < 0.001 ] = 0.001              ## avoid division
```

```
                             by zero
161              fsquare_minus_usquare_over_ucube = np.divide(  fsquare[1:m−1,1:n−1] −
                     u_old_square[1:m−1, 1:n−1] , u_old_cube[ 1:m−1, 1:n−1 ] )
162                  #
163                  u_new[ 1:m−1, 1:n−1 ]  +=  Delta_t*two_over_beta *
                     fsquare_minus_usquare_over_ucube;
164          case '2':           ## 2.  Le et al. method
165              umod = u_old[ 1:m−1, 1:n−1 ]
166              umod[ abs(umod) < 1e−3 ] = 1e−3;  ### avoid division by small number
167              u_new[ 1:m−1, 1:n−1 ]  +=  Delta_t*(1/beta) * ( np.divide( noisy_img[ 1:m
                     −1, 1:n−1 ] , umod ) − 1. )  ### check !
168          case _:              ## 3.  ROF method is default
169              u_new[ 1:m−1, 1:n−1 ]  +=  Delta_t*two_over_beta * (  noisy_img[ 1:m−1, 1:n
                     −1 ] − u_old[ 1:m−1, 1:n−1 ] )
170
171       u_old=u_new;
172    # end k−loop
173
174     ### test for goodness
175    denoised_img_small =  u_new[ 1:m−1, 1:m−1 ]
176    ###  td_mean_ratio_small =  std_mean_ratio( (1+w):(m−w),(1+w):(n−w) );
177    mymeas = np.abs ( orig_img_small − denoised_img_small );
178    mymeas1 = np.square( mymeas )
179    mymeas2 = np.square( orig_img_small )
180    MSE  = np.sum( mymeas ) / size_small;
181    RMSE = np.sqrt(MSE);
182    AD = np.sum( mymeas ) / size_small;
183    ##PSNR = 10*log10((255*255)/MSE)
184    ##SNR
185    ### SI = sum( std_mean_ratio_small(:) );1
186    ### SI = SI/(m−2*w);
187    ### SI = SI/(n−2*w)
188    Corr2 = np.corrcoef( orig_img_small.flatten(), denoised_img_small.flatten()  )[0,1]
                ## of diagonal matrix element
189    # UQI
190    mean_orig      = np.mean( orig_img_small.flatten() )
```

```
191     mean_denoised = np.mean( denoised_img_small.flatten() )

192     luminance      = 2*mean_orig*mean_denoised / (   mean_orig*mean_orig + mean_denoised*
            mean_denoised )

193     std_orig       = np.std(  orig_img_small.flatten() )

194     std_denoised = np.std( denoised_img_small.flatten() )

195     contrast       = 2*std_orig*std_denoised / (   std_orig*std_orig + std_denoised*
            std_denoised )

196     UQI            = Corr2 * luminance * contrast

197

198     #image display

199     strbeta =  "{:.1f}".format(beta); strRMSE = "{:.3f}".format(RMSE);        strAD = "{:.3f}
            ".format(AD);   strCorr2 = "{:.3f}".format(Corr2);   strUQI = "{:.3f}".format(UQI)

200     time_used = time.time() - cur_time

201     print("beta =", strbeta, ";   time used =", f"{time_used:.3f}", "seconds" , "\t;\t", "
            min. entry:", "{:.3f}".format( np.min(u_new) ), "  max. entry:", "{:.3f}".format(
            np.max( u_new )) ,

202                    " ; \t AD=", strAD, "  RMSE=", strRMSE, "  Corr=", strCorr2, "  UQI=",
                        strUQI   )

203     #

204     plt.imshow(u_new, cmap='gray')  ;   plt.title('Denoised by' + method + 'beta=' + strbeta
            ) ; plt.show();

205     #

206     outfilename = outfiledir + "/" + image_name + method + 'beta=' + strbeta + '_' +
            windowstext + '_RMSE=' + strRMSE + '_AD=' + strAD + '_corr2=' + strCorr2 + "
            _UQI=" + strUQI + '.bmp'

207

208     # write denoised image to outfiledir

209     cv2.imwrite(outfilename, u_new*255);

210

211     beta += beta_step;

212 #  end beta loop

213

214

215 print("*** DONE")
```
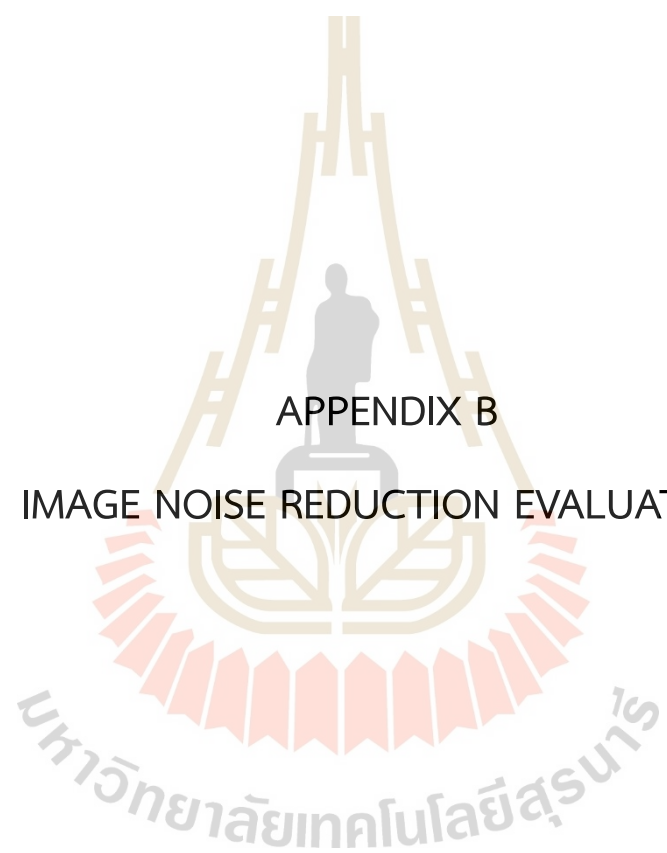
APPENDIX B

IMAGE NOISE REDUCTION EVALUATION

This chapter presents the data on image noise reduction evaluation using various β and λ parameters.

B.1 Image Quality Evaluation Results for β = 0.1

Table B.1 Table of evaluation images for various λ values for β=0.1.

λ	AD	RMSE	Corr	UQI
2.05	0.058	0.241	0.923	0.921
2.10	0.057	0.239	0.926	0.924
2.15	0.056	0.237	0.929	0.926
2.20	0.055	0.235	0.932	0.929
2.25	0.055	0.233	0.935	0.932
2.30	0.054	0.232	0.938	0.935
2.35	0.053	0.230	0.941	0.937
2.40	0.052	0.228	0.943	0.940
2.45	0.052	0.227	0.946	0.942
2.50	0.051	0.226	0.948	0.943
2.55	0.050	0.225	0.950	0.945
2.60	0.050	0.224	0.951	0.946
2.65	0.050	0.223	0.953	0.948
2.70	0.049	0.222	0.954	0.949
2.75	0.049	0.221	0.956	0.950
2.80	0.048	0.220	0.957	0.951
2.85	0.048	0.219	0.958	0.952
2.90	0.048	0.218	0.959	0.954
2.95	0.047	0.217	0.961	0.955
3.00	0.047	0.217	0.962	0.956
3.05	0.047	0.216	0.963	0.956
3.10	0.046	0.215	0.964	0.957
3.15	0.046	0.215	0.965	0.958
3.20	0.046	0.214	0.966	0.959
3.25	0.046	0.214	0.967	0.960
3.30	0.045	0.213	0.967	0.960
3.35	0.045	0.213	0.968	0.961
3.40	0.045	0.213	0.969	0.961
3.45	0.045	0.212	0.970	0.962
3.50	0.045	0.212	0.970	0.962
3.55	0.045	0.212	0.971	0.963
3.60	0.045	0.211	0.971	0.963
3.65	0.045	0.211	0.972	0.964
3.70	0.044	0.211	0.972	0.964
3.75	0.044	0.211	0.973	0.964
3.80	0.044	0.211	0.973	0.965

Table B.1 Table of evaluation images for various λ values for β=0.1 (Continued)

λ	AD	RMSE	Corr	UQI
3.85	0.044	0.210	0.974	0.965
3.90	0.044	0.210	0.974	0.965
3.95	0.044	0.210	0.974	0.965
4.00	0.044	0.210	0.975	0.966
4.05	0.044	0.210	0.975	0.966
4.10	0.044	0.210	0.975	0.966
4.15	0.044	0.210	0.976	0.966
4.20	0.044	0.210	0.976	0.967
4.25	0.044	0.210	0.976	0.967
4.30	0.044	0.210	0.976	0.967
4.35	0.044	0.210	0.977	0.967
4.40	0.044	0.210	0.977	0.967
4.45	0.044	0.210	0.977	0.967
4.50	0.044	0.210	0.977	0.967
4.55	0.044	0.210	0.977	0.968
4.60	0.044	0.210	0.978	0.968
4.65	0.044	0.210	0.978	0.968
4.70	0.044	0.210	0.978	0.968
4.75	0.044	0.210	0.978	0.968
4.80	0.044	0.210	0.978	0.968
4.85	0.044	0.210	0.978	0.968
4.90	0.044	0.210	0.978	0.968
4.95	0.044	0.210	0.978	0.968
5.00	0.044	0.210	0.979	0.968
5.05	0.044	0.210	0.979	0.968
5.10	0.044	0.210	0.979	0.968
5.15	0.044	0.210	0.979	0.968
5.20	0.044	0.210	0.979	0.968
5.25	0.044	0.210	0.979	0.968
5.30	0.044	0.210	0.979	0.968
5.35	0.044	0.210	0.979	0.968
5.40	0.044	0.210	0.979	0.968
5.45	0.044	0.210	0.979	0.968
5.50	0.044	0.210	0.979	0.968
5.55	0.044	0.210	0.979	0.968
5.60	0.044	0.210	0.979	0.968
5.65	0.044	0.211	0.980	0.968
5.70	0.044	0.211	0.980	0.968
5.75	0.044	0.211	0.980	0.968
5.80	0.044	0.211	0.980	0.968
5.85	0.044	0.211	0.980	0.968
5.90	0.044	0.211	0.980	0.968

Table B.1 Table of evaluation images for various λ values for β=0.1 (Continued)

λ	AD	RMSE	Corr	UQI
5.95	0.044	0.211	0.980	0.968
6.00	0.044	0.211	0.980	0.968
6.05	0.044	0.211	0.980	0.968
6.10	0.045	0.211	0.980	0.968
6.15	0.045	0.211	0.980	0.968
6.20	0.045	0.211	0.980	0.968
6.25	0.045	0.211	0.980	0.968
6.30	0.045	0.211	0.980	0.968
6.35	0.045	0.211	0.980	0.968
6.40	0.045	0.211	0.980	0.968
6.45	0.045	0.211	0.980	0.968
6.50	0.045	0.211	0.980	0.968
6.55	0.045	0.211	0.980	0.968
6.60	0.045	0.212	0.980	0.968
6.65	0.045	0.212	0.980	0.968
6.70	0.045	0.212	0.980	0.967
6.75	0.045	0.212	0.980	0.967
6.80	0.045	0.212	0.980	0.967
6.85	0.045	0.212	0.980	0.967
6.90	0.045	0.212	0.980	0.967
6.95	0.045	0.212	0.980	0.967
7.00	0.045	0.212	0.980	0.967
7.05	0.045	0.212	0.980	0.967
7.10	0.045	0.212	0.980	0.967
7.15	0.045	0.212	0.980	0.967
7.20	0.045	0.212	0.980	0.967
7.25	0.045	0.212	0.980	0.967
7.30	0.045	0.212	0.980	0.967
7.35	0.045	0.212	0.980	0.967
7.40	0.045	0.212	0.979	0.967
7.45	0.045	0.213	0.979	0.967
7.50	0.045	0.213	0.979	0.966
7.55	0.045	0.213	0.979	0.966
7.60	0.045	0.213	0.979	0.966
7.65	0.045	0.213	0.979	0.966
7.70	0.045	0.213	0.979	0.966
7.75	0.045	0.213	0.979	0.966
7.80	0.045	0.213	0.979	0.966
7.85	0.045	0.213	0.979	0.966
7.90	0.045	0.213	0.979	0.966
7.95	0.045	0.213	0.979	0.966
8.00	0.045	0.213	0.979	0.966

B.2 Image Quality Evaluation Results for β = 0.2

Table B.2 Table of evaluation images for various λ values for β=0.2.

λ	AD	RMSE	Corr	UQI
0.05	2.493	1.579	0.070	0.004
0.10	0.186	0.431	0.444	0.437
0.15	0.085	0.292	0.839	0.839
0.20	0.082	0.286	0.849	0.849
0.25	0.078	0.279	0.859	0.859
0.30	0.074	0.273	0.869	0.869
0.35	0.071	0.266	0.879	0.879
0.40	0.068	0.260	0.888	0.888
0.45	0.064	0.254	0.897	0.897
0.50	0.061	0.248	0.906	0.905
0.55	0.059	0.242	0.914	0.913
0.60	0.056	0.237	0.922	0.920
0.65	0.053	0.231	0.930	0.927
0.70	0.051	0.226	0.937	0.933
0.75	0.049	0.221	0.943	0.939
0.80	0.047	0.217	0.949	0.945
0.85	0.045	0.213	0.955	0.949
0.90	0.044	0.209	0.960	0.953
0.95	0.043	0.206	0.964	0.957
1.00	0.041	0.203	0.967	0.960
1.05	0.040	0.201	0.970	0.963
1.10	0.040	0.199	0.972	0.964
1.15	0.039	0.198	0.974	0.966
1.20	0.039	0.196	0.976	0.967
1.25	0.038	0.195	0.977	0.968
1.30	0.038	0.195	0.977	0.968
1.35	0.038	0.194	0.978	0.969
1.40	0.038	0.194	0.979	0.969
1.45	0.037	0.193	0.979	0.969
1.50	0.037	0.193	0.979	0.969
1.55	0.037	0.193	0.979	0.969
1.60	0.037	0.193	0.980	0.969
1.65	0.037	0.193	0.980	0.969
1.70	0.037	0.193	0.980	0.969
1.75	0.037	0.193	0.980	0.969
1.80	0.037	0.193	0.980	0.969
1.85	0.037	0.194	0.980	0.968
1.90	0.038	0.194	0.980	0.968
1.95	0.038	0.194	0.979	0.968
2.00	0.038	0.194	0.979	0.968

Table B.2 Table of evaluation images for various λ values for β=0.2 (Continued)

λ	AD	RMSE	Corr	UQI
2.05	0.038	0.194	0.979	0.967
2.10	0.038	0.195	0.979	0.967
2.15	0.038	0.195	0.979	0.967
2.20	0.038	0.195	0.979	0.967
2.25	0.038	0.195	0.979	0.966
2.30	0.038	0.196	0.979	0.966
2.35	0.038	0.196	0.978	0.966
2.40	0.038	0.196	0.978	0.966
2.45	0.039	0.196	0.978	0.965
2.50	0.039	0.197	0.978	0.965
2.55	0.039	0.197	0.978	0.965
2.60	0.039	0.197	0.978	0.964
2.65	0.039	0.197	0.977	0.964
2.70	0.039	0.198	0.977	0.964
2.75	0.039	0.198	0.977	0.964
2.80	0.039	0.198	0.977	0.963
2.85	0.039	0.198	0.977	0.963
2.90	0.039	0.199	0.977	0.963
2.95	0.040	0.199	0.976	0.963
3.00	0.040	0.199	0.976	0.962
3.05	0.040	0.199	0.976	0.962
3.10	0.040	0.200	0.976	0.962
3.15	0.040	0.200	0.976	0.961
3.20	0.040	0.200	0.976	0.961
3.25	0.040	0.200	0.975	0.961
3.30	0.040	0.201	0.975	0.961
3.35	0.040	0.201	0.975	0.960
3.40	0.040	0.201	0.975	0.960
3.45	0.041	0.201	0.975	0.960
3.50	0.041	0.202	0.974	0.960
3.55	0.041	0.202	0.974	0.959
3.60	0.041	0.202	0.974	0.959
3.65	0.041	0.202	0.974	0.959
3.70	0.041	0.202	0.974	0.959
3.75	0.041	0.202	0.974	0.958
3.80	0.041	0.203	0.973	0.958
3.85	0.041	0.203	0.973	0.958
3.90	0.041	0.203	0.973	0.958
3.95	0.041	0.203	0.973	0.957
4.00	0.041	0.204	0.973	0.957
4.05	0.042	0.204	0.973	0.957

B.3   Image Quality Evaluation Results for β = 0.3

Table B.3 Table of evaluation images for various λ values for β=0.3.

λ	AD	RMSE	Corr	UQI
0.05	0.182	0.427	0.381	0.378
0.10	0.080	0.282	0.854	0.854
0.15	0.072	0.268	0.876	0.875
0.20	0.065	0.255	0.895	0.895
0.25	0.058	0.242	0.913	0.912
0.30	0.053	0.230	0.929	0.926
0.35	0.048	0.220	0.942	0.938
0.40	0.044	0.211	0.953	0.948
0.45	0.042	0.204	0.962	0.955
0.50	0.039	0.198	0.969	0.961
0.55	0.038	0.194	0.973	0.965
0.60	0.037	0.192	0.976	0.967
0.65	0.036	0.190	0.978	0.968
0.70	0.036	0.190	0.979	0.969
0.75	0.036	0.189	0.979	0.969
0.80	0.036	0.190	0.979	0.968
0.85	0.036	0.190	0.979	0.968
0.90	0.036	0.190	0.979	0.968
0.95	0.036	0.191	0.979	0.967
1.00	0.037	0.191	0.978	0.966
1.05	0.037	0.192	0.978	0.966
1.10	0.037	0.193	0.978	0.965
1.15	0.037	0.193	0.977	0.965
1.20	0.038	0.194	0.977	0.964
1.25	0.038	0.194	0.977	0.963
1.30	0.038	0.195	0.976	0.963
1.35	0.038	0.196	0.976	0.962
1.40	0.038	0.196	0.976	0.962
1.45	0.039	0.197	0.975	0.961
1.50	0.039	0.197	0.975	0.960
1.55	0.039	0.198	0.974	0.960
1.60	0.039	0.198	0.974	0.959
1.65	0.040	0.199	0.974	0.959
1.70	0.040	0.199	0.973	0.958
1.75	0.040	0.200	0.973	0.958
1.80	0.040	0.200	0.973	0.957
1.85	0.040	0.201	0.972	0.957
1.90	0.040	0.201	0.972	0.956
1.95	0.041	0.201	0.971	0.956
2.00	0.041	0.202	0.971	0.955

B.4 Image Quality Evaluation Results for $\beta = 0.5$

Table B.4 Table of evaluation images for various λ values for β=0.5.

λ	AD	RMSE	Corr	UQI
0.05	0.074	0.271	0.870	0.870
0.10	0.055	0.235	0.920	0.918
0.15	0.044	0.209	0.952	0.947
0.20	0.038	0.195	0.970	0.962
0.25	0.036	0.189	0.977	0.967
0.30	0.036	0.188	0.978	0.967
0.35	0.036	0.190	0.978	0.966
0.40	0.037	0.191	0.977	0.965
0.45	0.037	0.193	0.976	0.963
0.50	0.038	0.194	0.975	0.961
0.55	0.038	0.196	0.974	0.960
0.60	0.039	0.197	0.973	0.958
0.65	0.039	0.199	0.972	0.957
0.70	0.040	0.200	0.971	0.955
0.75	0.040	0.201	0.970	0.954
0.80	0.041	0.202	0.969	0.953
0.85	0.041	0.203	0.968	0.952
0.90	0.042	0.204	0.968	0.950
0.95	0.042	0.205	0.967	0.949
1.00	0.042	0.206	0.966	0.948
1.05	0.043	0.207	0.965	0.947
1.10	0.043	0.207	0.964	0.946
1.15	0.043	0.208	0.963	0.945
1.20	0.044	0.209	0.963	0.944
1.25	0.044	0.209	0.962	0.943
1.30	0.044	0.210	0.961	0.942
1.35	0.044	0.211	0.961	0.941
1.40	0.045	0.211	0.960	0.940
1.45	0.045	0.212	0.959	0.939
1.50	0.045	0.212	0.959	0.938
1.55	0.045	0.213	0.958	0.937
1.60	0.045	0.213	0.958	0.937
1.65	0.046	0.214	0.957	0.936
1.70	0.046	0.214	0.956	0.935
1.75	0.046	0.214	0.956	0.934
1.80	0.046	0.215	0.955	0.934
1.85	0.046	0.215	0.955	0.933
1.90	0.046	0.215	0.954	0.933
1.95	0.047	0.216	0.954	0.932
2.00	0.047	0.216	0.953	0.931

B.5   Image Quality Evaluation Results for β = 0.8

Table B.5 Table of evaluation images for various λ values for β=0.8.

λ	AD	RMSE	Corr	UQI
0.05	0.048	0.219	0.939	0.935
0.10	0.036	0.189	0.976	0.965
0.15	0.036	0.191	0.977	0.965
0.20	0.038	0.195	0.975	0.961
0.25	0.039	0.198	0.972	0.957
0.30	0.041	0.201	0.970	0.953
0.35	0.042	0.204	0.967	0.950
0.40	0.042	0.206	0.965	0.947
0.45	0.043	0.208	0.963	0.944
0.50	0.044	0.210	0.961	0.942
0.55	0.045	0.211	0.960	0.940
0.60	0.045	0.212	0.958	0.938
0.65	0.046	0.213	0.957	0.936
0.70	0.046	0.215	0.955	0.934
0.75	0.046	0.215	0.954	0.932
0.80	0.047	0.216	0.953	0.931
0.85	0.047	0.217	0.952	0.929
0.90	0.047	0.217	0.951	0.928
0.95	0.047	0.218	0.950	0.927
1.00	0.048	0.218	0.949	0.926
1.05	0.048	0.219	0.949	0.925
1.10	0.048	0.219	0.948	0.925
1.15	0.048	0.220	0.947	0.924
1.20	0.048	0.220	0.947	0.923
1.25	0.048	0.220	0.946	0.922
1.30	0.049	0.220	0.946	0.922
1.35	0.049	0.221	0.946	0.921
1.40	0.049	0.221	0.945	0.921
1.45	0.049	0.221	0.945	0.920
1.50	0.049	0.221	0.944	0.920
1.55	0.049	0.221	0.944	0.919
1.60	0.049	0.221	0.944	0.919
1.65	0.049	0.222	0.944	0.919
1.70	0.049	0.222	0.943	0.918
1.75	0.049	0.222	0.943	0.918
1.80	0.049	0.222	0.943	0.918
1.85	0.049	0.222	0.943	0.918
1.90	0.049	0.222	0.943	0.917
1.95	0.049	0.222	0.942	0.917
2.00	0.049	0.222	0.942	0.917

B.6 Image Quality Evaluation Results for β = 1.0

Table B.6 Table of evaluation images for various λ values for β=1.0.

λ	AD	RMSE	Corr	UQI
0.05	0.038	0.196	0.967	0.959
0.10	0.037	0.191	0.977	0.964
0.15	0.039	0.197	0.973	0.958
0.20	0.041	0.202	0.969	0.952
0.25	0.042	0.206	0.966	0.948
0.30	0.044	0.209	0.962	0.943
0.35	0.045	0.211	0.960	0.940
0.40	0.045	0.213	0.957	0.936
0.45	0.046	0.215	0.955	0.934
0.50	0.047	0.216	0.953	0.931
0.55	0.047	0.217	0.952	0.929
0.60	0.047	0.218	0.950	0.927
0.65	0.048	0.219	0.949	0.926
0.70	0.048	0.219	0.948	0.925
0.75	0.048	0.220	0.947	0.923
0.80	0.048	0.220	0.946	0.922
0.85	0.049	0.221	0.946	0.921
0.90	0.049	0.221	0.945	0.921
0.95	0.049	0.221	0.945	0.920
1.00	0.049	0.221	0.944	0.919
1.05	0.049	0.222	0.944	0.919
1.10	0.049	0.222	0.943	0.918
1.15	0.049	0.222	0.943	0.918
1.20	0.049	0.222	0.942	0.917
1.25	0.049	0.222	0.942	0.917
1.30	0.049	0.222	0.942	0.917
1.35	0.050	0.223	0.942	0.916
1.40	0.050	0.223	0.942	0.916
1.45	0.050	0.223	0.942	0.916
1.50	0.050	0.223	0.941	0.916
1.55	0.050	0.223	0.941	0.916
1.60	0.050	0.223	0.941	0.916
1.65	0.050	0.223	0.941	0.915
1.70	0.050	0.223	0.941	0.915
1.75	0.050	0.223	0.941	0.915
1.80	0.050	0.223	0.941	0.915
1.85	0.050	0.224	0.941	0.915
1.90	0.050	0.224	0.941	0.914
1.95	0.050	0.224	0.941	0.914
2.00	0.050	0.224	0.941	0.914

CURRICULUM VITAE

NAME : Saruta Chong-Ngam   **GENDER :** Female

EDUCATION BACKGROUND:

- Bachelor of Science (Mathematics), Burapha University, Thailand, 2016

CONFERENCE:

- Jong-ngam, S., Tanthanuch, J., Schulz, E., Damnet, M., & Suriyavijitseranee, A. (2024). Statistical distribution analysis of signals in medical ultrasound images. In *Proceedings of the 7th National Academic Conference, Graduate School, Suan Sunandha Rajabhat University* (pp. 494–503). August 1, 2024.

EXPERIENCE:

- Teaching assistant in Suranaree University of Technology, Calculus I

- Served as part of the mathematics instructor team in a support and promotion program for Grade 12 students from Tha Song Yang Wittayakom School and Umphang Wittayakom School to prepare for entrance exams in medical and related health science fields.